Global Generic Dynamics Close to Symmetry

Isabel S. Labouriau   Alexandre A. P. Rodrigues
Centro de Matemática da Universidade do Porto *
and Faculdade de Ciências, Universidade do Porto
Rua do Campo Alegre, 687, 4169-007 Porto, Portugal
islabour@fc.up.pt   alexandre.rodrigues@fc.up.pt

Keywords:
Heteroclinic networks, Symmetry breaking, Bykov cycles, Shilnikov's homoclinic cycles

AMS Subject Classifications:
Primary: 34C28; Secondary: 34C37, 37C29, 37D05, 37G35

Abstract

Our object of study is the dynamics that arises in generic perturbations of an asymptotically stable heteroclinic cycle in $\mathbf{S}^3$. The cycle involves two saddle-foci of different type and is structurally stable within the class of $(\mathbf{Z}_2 \oplus \mathbf{Z}_2)$–symmetric vector fields. The cycle contains a two-dimensional connection that persists as a transverse intersection of invariant surfaces under symmetry-breaking perturbations.

Gradually breaking the symmetry in a two-parameter family we get a wide range of dynamical behaviour: an attracting periodic trajectory; other heteroclinic trajectories; homoclinic orbits; n-pulses; suspended horseshoes and cascades of bifurcations of periodic trajectories near an unstable homoclinic cycle of Shilnikov type. We also show that, generically, the coexistence of linked homoclinic orbits at the two saddle-foci has codimension 2 and takes place arbitrarily close to the symmetric cycle.

1 Introduction

Symmetry, exact or approximate, plays an important role in the analysis of non-linear physical systems. Reflectional and rotational symmetries, for instance, are relevant to a wide range of experiments in physics, with the canonical example arising in the context of rotating Rayleigh–Bénard convection [8]; see also Melbourne *et al* [33]. Models are first constructed with perfect symmetry, leading to the existence of invariant subspaces and thus to the existence of heteroclinic cycles and networks and their robustness with respect to symmetric perturbations. Equivariant bifurcation theory developed by several authors (see for instance Golubitsky *et al* [21]) has produced results that agree well with physical systems.

Nevertheless, reality usually has less perfect symmetry. Thus it would be desirable to understand the dynamics that persists under small symmetry-breaking perturbations. In the context of equivariant dynamics, it corresponds to the explicit addition of specific terms that break the symmetry of the system — *forced symmetry-breaking*. This is the subject of the present article.

*CMUP is supported by the European Regional Development Fund through the programme COMPETE and by the Portuguese Government through the Fundação para a Ciência e a Tecnologia (FCT) under the project PEst-C/MAT/UI0144/2011. A.A.P. Rodrigues was supported by the grant SFRH/BD/28936/2006 of FCT.

In the space of all smooth vector fields on $\mathbf{R}^n$ endowed with the C^1 Whitney topology and the topological equivalence, a vector field is structurally stable if it belongs to the interior of its equivalence class. The set of non-structurally stable systems is called the *bifurcation set* and the study of its structure is a big challenge; even for differential equations in three dimensions, the structure of the bifurcation set might be very complicated. Symmetric vector fields are not structurally stable and provide a good starting point for this study.

Particular effects of small symmetry-breaking have already been studied by several authors and aspects related to the question of how much of the dynamics persists under the inclusion of small noise have also been considered. However details vary greatly between the different examples. For instance, Kirk and Rucklidge [28] consider small symmetry-breaking for a system with an asymptotically stable heteroclinic network, Chossat [13] investigates the effect of symmetry-breaking near a symmetric homoclinic cycle and Melbourne [32] analyses small perturbations near a system whose dynamics contains a heteroclinic cycle between three symmetric periodic solutions (associated to non-trivial closed trajectories).

The construction of explicit examples of vector fields whose flow has asymptotically stable heteroclinic networks has been done by Aguiar *et al* [4] and Rodrigues *et al* [36]; adding terms that break the symmetry, the authors found examples with spontaneous bifurcation to chaos. This route to chaos corresponds to an interaction of symmetry-breaking, robust switching and chaotic cycling.

In this article, we study the dynamics observed in a $(\mathbf{Z}_2 \oplus \mathbf{Z}_2)$–symmetric system in $\mathbf{S}^3$; we look at properties that persist under symmetry-breaking perturbations and we characterize the set of non-wandering points. Our results appeal to generic properties of the system and are valid for any $(\mathbf{Z}_2 \oplus \mathbf{Z}_2)$– equivariant system satisfying these properties. This analysis was partially motivated by a system constructed by Aguiar [2], whose flow contains a heteroclinic network connecting two saddle-foci of different types, where one heteroclinic connection is one-dimensional and the other is two-dimensional and both lie in different fixed point subspaces.

Our work also forms part of a program, started by Bykov [9] in the eighties, of systematic study of the dynamics near networks of equilibria whose linearization has a pair of non-real eigenvalues — *rotating equilibria.*

The main results of the article are stated in section 2. To make the paper self contained and readable, we recall some definitions and results about equivariance, heteroclinic switching and homo/heteroclinic bifurcations, adapted to our interests.

We consider a smooth two-parameter family of vector fields f on $\mathbf{R}^n$ with flow given by the unique solution $x(t) = \varphi(t, x_0) \in \mathbf{R}^n$ of

$$\dot{x} = f(x, \lambda_1, \lambda_2) \qquad x(0) = x_0, \tag{1.1}$$

where λ_1 and λ_2 are real parameters.

Given two hyperbolic equilibria A and B, an m-dimensional *heteroclinic connection* from A to B, denoted $[A \to B]$, is an m-dimensional connected and flow-invariant manifold contained in $W^u(A) \cap W^s(B)$. There may be more than one connection from A to B.

Let $\mathcal{S} = \{A_j : j \in \{1, \ldots, k\}\}$ be a finite ordered set of hyperbolic equilibria. We say that there is a *heteroclinic cycle* associated to $\mathcal{S}$ if

$$\forall j \in \{1, \ldots, k\}, W^u(A_j) \cap W^s(A_{j+1}) \neq \emptyset \pmod{k}.$$

If $k = 1$ we say that there is a *homoclinic cycle* associated to A_1. In other words, there is a connection whose trajectories tend to A_1 in both backward and forward time. A *heteroclinic network* is a connected set consisting of a finite union of heteroclinic cycles.

Heteroclinic networks appear frequently in the context of symmetry. Given a compact Lie group Γ acting linearly on $\mathbf{R}^n$, a vector field f is $\Gamma-$equivariant if for all $\gamma \in \Gamma$ and $x \in \mathbf{R}^n$, we have $f(\gamma x) = \gamma f(x)$. In this case $\gamma \in \Gamma$ is said to be a symmetry of f and all elements of the subgroup $\langle\gamma\rangle$ generated by γ are also symmetries of f. We refer the reader to Golubitsky, Stewart and Schaeffer [21] for more information on differential equations with symmetry.

The Γ-*orbit* of $x_0 \in \mathbf{R}^n$ is the set $\Gamma(x_0) = \{\gamma x_0, \gamma \in \Gamma\}$. If x_0 is an equilibrium of (1.1), so are the elements in its Γ-orbit.

The *isotropy subgroup* of $x_0 \in \mathbf{R}^n$ is $\Gamma_{x_0} = \{\gamma \in \Gamma, \quad \gamma x_0 = x_0\}$. For an isotropy subgroup Σ of Γ, its *fixed point subspace* is

$$Fix(\Sigma) = \{x \in \mathbf{R}^n : \forall \gamma \in \Sigma, \gamma x = x\}.$$

If f is Γ-equivariant and Σ is an isotropy subgroup, then $Fix(\Gamma)$ is a flow-invariant vector space. This is the reason for the persistence of heteroclinic networks in symmetric flows: connections taking place inside a flow-invariant subspace may be robust to perturbations that preserve this subspace, even though they may be destroyed by more general perturbations.

2 Statement of Results

2.1 Description of the problem

The starting point of the analysis is a differential equation on the unit sphere $\mathbf{S}^3 \subset \mathbf{R}^4$

$$\dot{x} = f_0(x) \tag{2.2}$$

where $f_0 : \mathbf{S}^3 \to \mathbf{TS}^3$ is a smooth[1] vector field with the following properties:

(P1) The organizing centre f_0 is equivariant under the action of $\Gamma = \mathbf{Z}_2 \oplus \mathbf{Z}_2$ on $\mathbf{S}^3$ induced by the action on $\mathbf{R}^4$ of

$$\gamma_1(x_1, x_2, x_3, x_4) = (-x_1, -x_2, x_3, x_4)$$

and

$$\gamma_2(x_1, x_2, x_3, x_4) = (x_1, x_2, -x_3, x_4).$$

From now on, for a subgroup Δ of Γ, we denote by $Fix(\Delta)$ the sphere

$$\{x \in \mathbf{S}^3 : \delta x = x, \forall \delta \in \Delta\}.$$

In particular,

$$Fix(\Gamma) = \{(0, 0, 0, 1) \equiv \mathbf{v}, (0, 0, 0, -1) \equiv \mathbf{w}\}\ .$$

(P2) The equilibria $\mathbf{v}$ and $\mathbf{w}$ in $Fix(\Gamma)$ are hyperbolic saddle-foci where the eigenvalues of $df_0|_{x=X}$ are:

- $-C_\mathbf{v} \pm \alpha_\mathbf{v} i$ and $E_\mathbf{v}$ with $\alpha_\mathbf{v} \neq 0$, $C_\mathbf{v} > E_\mathbf{v} > 0$ for $X = \mathbf{v}$
- $E_\mathbf{w} \pm \alpha_\mathbf{w} i$ and $-C_\mathbf{w}$ with $\alpha_\mathbf{w} \neq 0$, $C_\mathbf{w} > E_\mathbf{w} > 0$ for $X = \mathbf{w}$.

(P3) Within $Fix(\langle\gamma_1\rangle)$ the only equilibria are $\mathbf{v}$ and $\mathbf{w}$, a source and a sink, respectively. It follows that there are two heteroclinic trajectories ($\langle\gamma_2\rangle$-symmetric) from $\mathbf{v}$ to $\mathbf{w}$ (see case (a) of figure 1) that we denote by $[\mathbf{v} \to \mathbf{w}]$.

(P4) Within $Fix(\langle\gamma_2\rangle)$ the only equilibria are $\mathbf{v}$ and $\mathbf{w}$, a sink and a source, respectively. Thus, there is a two-dimensional heteroclinic connection from $\mathbf{w}$ to $\mathbf{v}$ (see case (b) of figure 1). This connection together with the equilibria is the two-sphere $Fix(\langle\gamma_2\rangle)$.

[1]By smooth we mean a map of class C^k, for a large enough k. In most places, C^1 suffices.

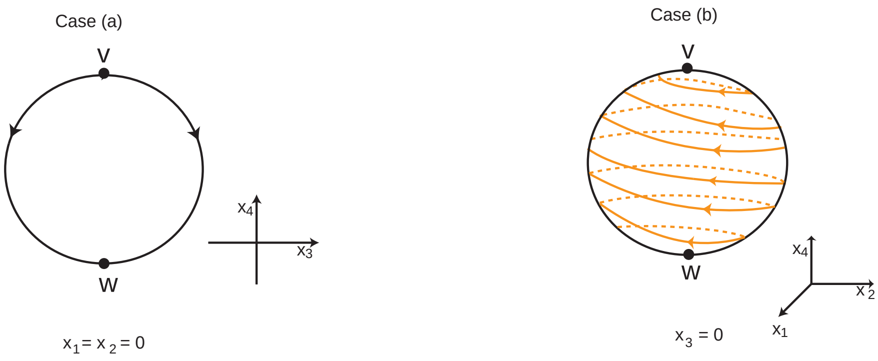

Figure 1: Heteroclinic connections for the organizing center f_0. (a) From properties (P1)–(P3), the invariant circle $Fix(\langle\gamma_1\rangle)$ consists of the two equilibria $\mathbf{v}$ and $\mathbf{w}$ and two trajectories connecting them. (b) The invariant sphere $Fix(\langle\gamma_2\rangle)$ forms a two-dimensional connection $[\mathbf{w} \to \mathbf{v}]$ by property (P4). The arrows represent the coordinate system in which the heteroclinic connections lie.

Our object of study is a germ at $(\lambda_1, \lambda_2) = (0, 0)$ of a two-parameter family of vector fields of $f(., \lambda_1, \lambda_2)$ that unfolds the symmetry-breaking of the organizing center $f_0(x) = f(x, 0, 0)$. We denote by f any of the vector fields

$$x \mapsto f(x, \lambda_1, \lambda_2),$$

when the choice of λ_1 and λ_2 is clear from the context. The parameters λ_1 and λ_2 control the type of symmetry-breaking. Specifically, if $\lambda_1 \neq 0$, we are perturbing the $(\mathbf{Z}_2 \oplus \mathbf{Z}_2)$–equivariant vector field by breaking the symmetry γ_2 and preserving γ_1 (see Table 1). Analogously, if $\lambda_2 \neq 0$, we destroy the equivariance under γ_1 and preserve γ_2. Throughout this article, we are assuming that these parameters act independently.

Since $\mathbf{v}$ and $\mathbf{w}$ are hyperbolic equilibria, then for each λ_1 and λ_2 close to 0, the vector field f still has two equilibria with eigenvalues satisfying (P2). When there is no loss of generality we ignore their dependence on λ_1 and λ_2. In particular, the dimensions of the local stable and unstable manifolds of $\mathbf{v}$ and $\mathbf{w}$ do not change, but generically the heteroclinic connections may be destroyed, since the fixed point subsets are no longer flow-invariant. More precisely, we are assuming:

(P5) Depending on the values of λ_1 and λ_2, the vector field f has the symmetries indicated in Table 1.

Parameters	Symmetries preserved	Symmetries broken
$\lambda_1 = \lambda_2 = 0$	$\mathbf{Z}_2 \oplus \mathbf{Z}_2$	none
$\lambda_1 \neq 0$ and $\lambda_2 = 0$	$\langle\gamma_1\rangle$	$\langle\gamma_2\rangle$
$\lambda_1 = 0$ and $\lambda_2 \neq 0$	$\langle\gamma_2\rangle$	$\langle\gamma_1\rangle$
$\lambda_1 \neq 0$ and $\lambda_2 \neq 0$	Identity	$\mathbf{Z}_2 \oplus \mathbf{Z}_2$

Table 1: The type of symmetry breaking depends on the parameters.

The following property states that the invariant manifolds $W^u(\mathbf{w})$ and $W^s(\mathbf{v})$ meet transversely. Generically, the intersection of the manifolds consists of a finite number of trajectories.

(P6) **[Transversality]** For $\lambda_1 \neq 0$, the two-dimensional manifolds $W^u(\mathbf{w})$ and $W^s(\mathbf{v})$ intersect transversely at a finite number of trajectories.

(P7) **[Non-degeneracy]** For $\lambda_2 \neq 0$, the heteroclinic connections $[\mathbf{v} \to \mathbf{w}]$ are broken.

Note that (P1)–(P4) are satisfied on a C^1–open subset of smooth Γ–equivariant vector fields on $\mathbf{S}^3$ and that (P5)–(P7) hold for a C^1–open subset of two parameter families of vector fields unfolding a Γ–equivariant differential equation on the sphere. Our results are still valid on any manifold C^1–diffeomorphic to $\mathbf{S}^3$ if instead of (P1) we assume that f_0 commutes with two involutions γ_1 and γ_2 that fix, respectively, a circle and a two-sphere, that only meet at $\{\mathbf{v}, \mathbf{w}\}$.

2.2 Organizing centre

When $\lambda_1 = \lambda_2 = 0$, there is a heteroclinic network (that we denote by Σ), in $\mathbf{S}^3$, associated to the two saddle-foci $\mathbf{v}$ and $\mathbf{w}$. The network Σ is the union of two heteroclinic cycles related by the γ_2–symmetry.

In order to describe the dynamics near Σ when the symmetry is broken, we start breaking part of the symmetry, as outlined in Table 2.

Parameters	$\dim([\mathbf{v} \to \mathbf{w}])$	$\dim([\mathbf{w} \to \mathbf{v}])$	Section
$\lambda_1 = \lambda_2 = 0$	1	2	2.2
$\lambda_1 \neq 0$ and $\lambda_2 = 0$	1	1	4 and 2.3
$\lambda_1 = 0$ and $\lambda_2 \neq 0$	Not defined	2	5 and 2.4
$\lambda_1 \neq 0$ and $\lambda_2 \neq 0$	Not defined	1	6 and 2.5

Table 2: Dependence of heteroclinic connections on the symmetry and on the parameters.

The heteroclinic connections in the network are contained in fixed point subspaces such that the hypothesis (H1) of Krupa & Melbourne [30] is satisfied. Since the inequality $C_\mathbf{v} C_\mathbf{w} > E_\mathbf{v} E_\mathbf{w}$ holds, the Krupa and Melbourne stability criterion ([30]) may be applied to Σ and we have:

Proposition 1 *Under conditions (P1)–(P4) the heteroclinic network Σ associated to $\mathbf{v}$ and $\mathbf{w}$ is asymptotically stable.*

The previous result means that there exists an open neighbourhood V_Σ of the network Σ such that every trajectory starting in V_Σ is forward asymptotic to the network. Due to the $\langle\gamma_2\rangle$-equivariance, trajectories whose initial condition starts outside the invariant subspaces will approach in positive time one of the cycles. The time spent near each equilibrium increases geometrically. The ratio of this geometrical series is related to the eigenvalues of $df_0(x, 0, 0)$ at the equilibria. The fixed point hyperplanes prevent jumps between the two cycles; in particular, random visits to both cycles require breaking the symmetry (and thus the breaking of the invariant subspaces).

2.3 Breaking the two-dimensional connection

When (P6) holds with $\lambda_2 = 0$ and $\lambda_1 \neq 0$ the network $\Sigma^\star$ consists of two copies of the simplest heteroclinic cycle between two saddle-foci, where one heteroclinic connection is structurally

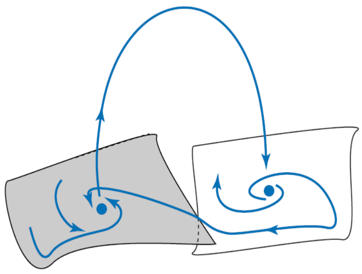

Figure 2: Bykov cycle: heteroclinic cycle associated to two saddle-foci of different types, in which the one-dimensional invariant manifolds coincide and the two-dimensional invariant manifolds have a transverse intersection.

stable and the other is not. This cycle, called a *Bykov cycle*, has been first studied in the eighties by Bykov [9] and by Glendinning and Sparrow [20].

A *Bykov cycle* is a cycle with two saddle-foci of different types, in which the one-dimensional invariant manifolds coincide and the two-dimensional invariant manifolds have a transversal intersection (see figure 2). It arises as a bifurcation of codimension 2. In the $\mathbf{Z}_2$–symmetric context, Bykov cycles are generic. The study of bifurcations arising in the unfolding *Bykov cycles*, called also T–points in the literature is done in [14]. We also refer Knobloch *et al* [29] who study heteroclinic cycles similar to $\Sigma^\star$ in the context of hamiltonian systems with one transverse intersection.

Recently, there has been a renewal of interest in this type of heteroclinic bifurcation in different contexts – see Sánchez *et al* [15], Homburg and Natiello [24], Ibáñez and Rodriguez [25]. Heteroclinic bifurcations of this type have also been reported to arise on models of Josephson junctions [11] and Michelson system [12]. Our approach is similar to that of Lamb *et al* [31], although they study $\mathbf{Z}_2$–reversible systems and we study the $\langle\gamma_1\rangle$-equivariant case and then break the symmetry.

There are two different possibilities for the geometry of the flow around $\Sigma^\star$, depending on the direction trajectories turn around the connection $[\mathbf{v} \to \mathbf{w}]$. Throughout this article, we only consider the case where each trajectory when close to $\mathbf{v}$ turns in the same direction as when close to $\mathbf{w}$. A simpler formulation of this will be given in Section 3.1 below, after we have established some notation, but for the moment we are assuming:

(P8) There are open neighbourhoods V and W of $\mathbf{v}$ and $\mathbf{w}$, respectively, such that, for any trajectory going from V to W, the direction of its turning around the connection $[\mathbf{v} \to \mathbf{w}]$ is the same in V and in W (see figure 3).

This is the situation in the reversible case studied by Lamb *et al* [31], where the anti-symmetry is a rotation by π. The condition would not hold if the anti-symmetry were a reflection.

In a more general setting the dynamics around heteroclinic cycles has been studied by Aguiar *et al* [5]. The main result of [5] is that, close to what remains of the network Σ after perturbation, there are trajectories that visit neighbourhoods of the saddles following all the heteroclinic connections in any given order. This is the concept of heteroclinic switching; the next paragraph gives a set-up of *switching* near a heteroclinic network. Recently, Homburg and Knobloch [23] gave an equivalent definition of switching for a heteroclinic network, using the notion of connectivity matrix (which characterizes the admissible sequences) and symbolic dynamics.

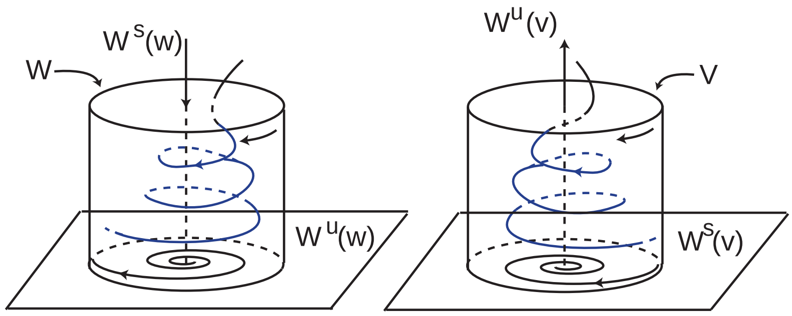

Figure 3: There are two different possibilities for the geometry of the flow around $\Sigma^\star$ depending on the direction trajectories turn around the heteroclinic connection $[\mathbf{v} \to \mathbf{w}]$. Throughout this paper, we restrict our study to the case where the direction of turning around $[\mathbf{v} \to \mathbf{w}]$ is the same in V and W.

For a heteroclinic network Σ with node set $\mathcal{A}$, a *path of order k* on Σ is a finite sequence $s^k = (c_j)_{j\in\{1,\ldots,k\}}$ of connections $c_j = [A_j \to B_j]$ in Σ such that $A_j, B_j \in \mathcal{A}$ and $B_j = A_{j+1}$ *i.e.* $c_j = [A_j \to A_{j+1}]$. For an infinite path, take any $j \in \mathbf{N}$.

Let N_Σ be a neighbourhood of the network Σ and let U_A be a neighbourhood of each node A in Σ. For each heteroclinic connection in Σ, consider a point p on it and a small neighbourhood V of p. The neighbourhoods of the nodes should be pairwise disjoint, as well for those of points in connections. Given neighbourhoods as above, the point q, or its trajectory $\varphi(t)$, *follows* the finite path $s^k = (c_j)_{j\in\{1,\ldots,k\}}$ of order k, if there exist two monotonically increasing sequences of times $(t_i)_{i\in\{1,\ldots,k+1\}}$ and $(z_i)_{i\in\{1,\ldots,k\}}$ such that for all $i \in \{1,\ldots,k\}$, we have $t_i < z_i < t_{i+1}$ and:

- $\varphi(t) \subset N_\Sigma$ for all $t \in (t_1, t_{k+1})$;
- $\varphi(t_i) \in U_{A_i}$ and $\varphi(z_i) \in V_i$ and
- for all $t \in (z_i, z_{i+1})$, $\varphi(t)$ does not visit the neighbourhood of any other node except that of A_{i+1}.

There is *finite switching* near Σ if for each finite path there is a trajectory that follows it. Analogously, we define *infinite* switching near Σ by requiring that each infinite path is followed by a trajectory. In other words, for any given forward infinite sequence of heteroclinic connections $(c_j)_{j\in\mathbf{N}}$ such that the ω-limit of any point in c_j coincide with the α-limit of any points in c_{j+1}, there exists at least one trajectory that remains very close to the network and follows the sequence (see figure 4).

Proposition 2 *If a vector field f_0 satisfies (P1)–(P4) and (P8), then the following properties are satisfied by all vector fields in an open neighbourhood of f_0 in the space of $\langle\gamma_1\rangle$-equivariant vector fields of class C^1 on $\mathbf{S}^3$:*

1. *the only heteroclinic connections from $\mathbf{v}$ to $\mathbf{w}$ are the original ones;*
2. *there are no homoclinic connections;*
3. *there is infinite switching;*
4. *the finite switching may be realized by an n-pulse heteroclinic connection $[\mathbf{w} \to \mathbf{v}]$;*

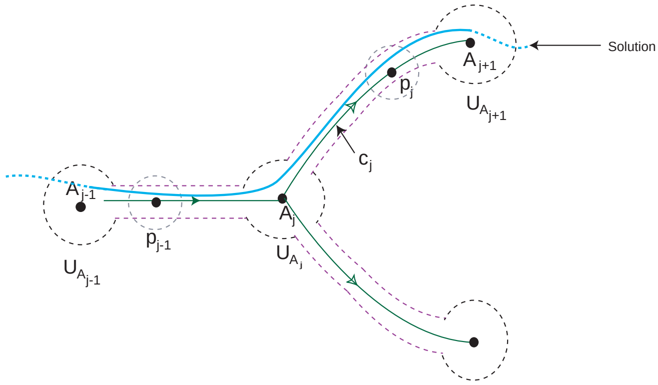

Figure 4: Trajectory shadowing two heteroclinic connections.

5. *there exists an increasing nested chain of suspended uniformly hyperbolic compact sets $(G_i)_{i\in\mathbf{N}}$ topologically conjugate to a full shift over a finite number of symbols, which accumulates on the cycle (see figure 5).*

In the restriction to a uniformly hyperbolic invariant compact set whose existence is assured by item 5 of proposition 2, the dynamics is conjugated to a full shift over a finite alphabet. In particular, since the ceiling function associated to the suspension of any horseshoe is bounded above and below (in a compact set), it follows that the topological entropy of the corresponding flow is positive. This means that there is a positive exponential growth rate for the number of orbits, for the first return map, distinguishable with fine but finite precision – see Abramov [1] and Katok [26].

The nested chain of horseshoes is illustrated in figure 5: a vertical rectangle in the wall of V, later called $H^{in}_{\mathbf{v}}$, first returns to the wall as several rectangles transverse to the original one. If the height of the rectangle is increased by moving its lower boundary closer to $W^s(\mathbf{v})$, then the number of returning rectangles (*legs* of the horseshoe) increases; continuing the rectangle all the way down to $W^s(\mathbf{v})$ creates infinitely many legs.

A challenge in topological dynamics is to decide whether periodic solutions can be separated by homotopies, or not. Roughly speaking, a *link* is a collection of disjoint one-spheres in $\mathbf{S}^3$. A *knot* is a link with one connected component. Two links $\mathcal{L}_1 \subset \mathbf{S}^3$ and $\mathcal{L}_2 \subset \mathbf{S}^3$ are equivalent if there exists an isotopy $\{\mathcal{H}_t\}_{t\in[0,1]}$ of $\mathbf{S}^3$ such that $\mathcal{H}_0 = Id_{\mathbf{S}^3}$ and $\mathcal{H}_1(\mathcal{L}_1) = \mathcal{L}_2$. We may use the following result:

Theorem 3 (Franks and Williams [16], 1985) *If Φ_t is a C^r flow on $\mathbf{R}^3$ or $\mathbf{S}^3$ such that either:*

- *$r > 1$ and Φ_t has a hyperbolic periodic orbit with a transverse homoclinic point, or*
- *$r > 2$ and Φ_t has a compact invariant set with positive topological entropy,*

then among the closed orbits there are infinitely many distinct knot types.

It follows that among all the closed orbits which appear in the nested chain of horseshoes, there are many distinct inequivalent knot types. In particular, we may conclude that:

Corollary 4 *If a vector field f_0 satisfies (P1)–(P4) and (P8) then, for the flow associated to all vector fields in an open neighbourhood of f_0 in the space of $\langle\gamma_1\rangle$–equivariant vector fields of*

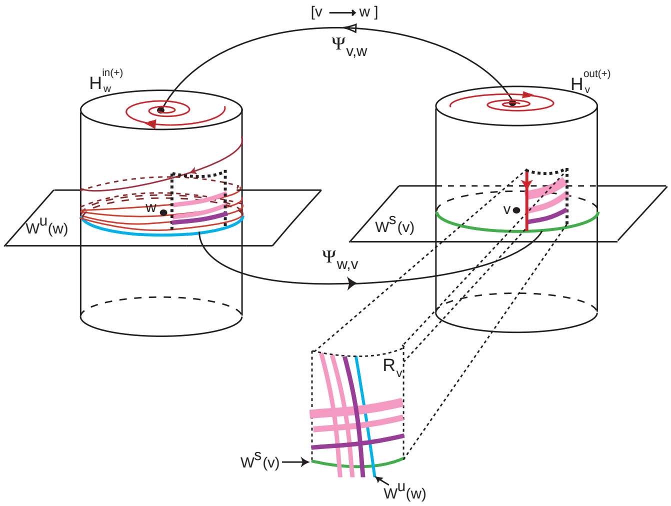

Figure 5: The presence of a transverse intersection creates a nested chain of uniformly hyperbolic horseshoes, which is accumulating on the cycle. Observe that horizontal strips s_i and their first return images by $\Psi_{\mathbf{w},\mathbf{v}} \circ \Phi_{\mathbf{w}} \circ \Psi_{\mathbf{v},\mathbf{w}} \circ \Phi_{\mathbf{v}}$ intersect in a transverse way.

class C^1 on $\mathbf{S}^3$, there are closed orbits linked to each of the cycles in $\Sigma^\star$ exhibiting infinitely many knot types.

The previous result shows that among all the periodic solutions, there are many distinct inequivalent knot types. Nevertheless, we do not know if these horseshoes induce all link types. For example, neither the standard horseshoe (with two strips) nor its second iterate induces all types of links. The third iterate of the Smale horseshoe induces all link types - see Kin [27]. Based on the paper of Hirasawa and Kin [22], we solved affirmatively the problem using the concepts of *generalized horseshoes* and *twist signature*.

Corollary 5 *If a vector field f_0 satisfies (P1)–(P4) and (P8) then, for the flow associated to all vector fields in an open neighbourhood of f_0 in the space of $\langle\gamma_1\rangle$–equivariant vector fields of class C^1 on $\mathbf{S}^3$, there are closed orbits linked to each of the cycles in $\Sigma^\star$ inducing all link types.*

We address the proof of corollary 5 in section 4. Observe that for each n–pulse heteroclinic connection from $\mathbf{w}$ to $\mathbf{v}$, we may define a *new* n-heteroclinic cycle and thus a *subsidiary Bykov cycle*. Hence, these *new* cycles have the same structure in their unfolding as the original cycles.

In the context of a heteroclinic cycle associated to non-trivial periodic solutions, Rodrigues *et al* [36] describe the phenomenon of *chaotic cycling*: there are trajectories that follow the cycle making any prescribed number of turns near the periodic solutions, for any given bi-infinite sequence of turns. The rigorous definition of this concept requires an open neighbourhood $V_{\Sigma^\star}$ of $\Sigma^\star$, a set of neighbourhoods of the saddles (isolating blocks) and a set of Poincaré sections near each limit cycle (counting sections). Given these sets, it is possible to code with an infinite word over a finite alphabet each trajectory that remains inside V_Σ for all time. Each repetition of a letter corresponds to a new turn inside the neighbourhood of the limit cycle; an infinite repetition (resp. periodic word) corresponds to a trajectory lying in an invariant manifold (resp. periodic solution). Coding trajectories that remain for all time in the neighbourhood of $\Sigma^\star$ is beyond the scope of this paper, but we point out that this technique may be naturally applied to a heteroclinic cycle of saddle-foci.

2.4 Breaking the one-dimensional connection

For C^1–vector fields on the plane, let Θ be an attracting heteroclinic network associated to two equilibria with two cycles sharing one connection. Assuming that ξ is the splitting parameter governing the common connection, it follows by Andronov-Leontovich theorem [6] that for sufficiently small $\xi > 0$ there exists a unique stable hyperbolic limit cycle such that when $\xi \to 0$, the limit cycle approaches the locus of one of the cycles of Θ and its period tends to $+\infty$.

The classical Shilnikov problem [38] in smooth three-dimensional systems states that small C^1–perturbations of an attracting homoclinic cycle associated to a saddle-focus could yield a stable hyperbolic periodic solution with the same properties of that of Andronov-Leontovich on the plane. The main goal of this section is to extend the classical Shilnikov problem for Bykov cycles. The technique to tackle our problem is similar to that of Shilnikov: the reduction to the Poincaré map.

When (P7) holds, with $\lambda_1 = 0$ and $\lambda_2 \neq 0$, the heteroclinic cycles that existed in the fully symmetric case disappear. The invariance of $Fix(\langle\gamma_2\rangle)$ is not preserved and the asymptotically stable heteroclinic network Σ is broken; nevertheless near the ghost of the original attractor there will still exist some attracting structure.

We will prove that each cycle is replaced by an asymptotically stable closed trajectory that lies near the original (attracting) heteroclinic cycle. One possibility would be to generate a *multi-pulse* heteroclinic connection from $\mathbf{v}$ to $\mathbf{w}$, that goes several times around close to where the original heteroclinic connection was, in a sense that will be made precise in Section 5. This is ruled out by the next result, proved in Section 5.

Theorem 6 *If a vector field f_0 satisfies (P1)–(P4), then the following properties are satisfied by all vector fields in an open neighbourhood of f_0 in the space of $\langle\gamma_2\rangle$–equivariant vector fields of class C^1 on $\mathbf{S}^3$:*

1. *there are no multi-pulse heteroclinic connections from $\mathbf{v}$ to $\mathbf{w}$;*
2. *near each of the two cycles present in the $(\mathbf{Z}_2 \oplus \mathbf{Z}_2)$–symmetric equation, the perturbed equations have a non-trivial asymptotically stable periodic solution.*

In our context, Theorem 6 may be rephrased as follows: consider a generic $\langle\gamma_2\rangle$-equivariant one-parameter perturbation $f(x, \lambda_2)$ of the $(\mathbf{Z}_2 \oplus \mathbf{Z}_2)$–symmetric organizing centre f_0 that satisfies (P7). Then, for each small $\lambda_2 \neq 0$ there is a pair of symmetry-related non-trivial asymptotically stable periodic solutions to $\dot{x} = f(x, 0, \lambda_2)$. As λ_2 tends to 0 the closed trajectories approach the two cycles in Σ and their period tends to $+\infty$. In local coordinates (such as will be assured by Samovol's Theorem, see Section 3 below), the limit cycle of the stable periodic trajectory winds increasingly around the local stable manifold of $\mathbf{w}$ and the time of flight inside fixed neighbourhoods of $\mathbf{v}$ and of $\mathbf{w}$ tends to $+\infty$.

2.5 Breaking the two heteroclinic connections

In this section we conclude that the Bykov cycle involving $\mathbf{v}$ and $\mathbf{w}$ may give rise to homoclinic orbits involving saddle-focus. These homoclinic cycles are usually called *Shilnikov homoclinic orbits* because the systematic study of the dynamics near them began with L. P. Shilnikov [38] in 1965. The homoclinic orbits associated to a saddle-focus is one of the main sources of chaotic dynamics in three-dimensional flows. In several applications these homoclinicities play an important role – see for example [10] in the setting of neuron model.

First of all, note that under perturbation the generalized horseshoes $(G_i)_{i\in\mathbf{N}}$ which occur near the Bykov cycle in proposition 2 survive for finitely many N. For each N, G_N is uniformly hyperbolic but $\bigcup_{i\in\mathbf{N}} G_i$ is not.

2.5.1 Dynamics near Shilnikov Homoclinic Orbits

In autonomous planar systems, a codimension 1 homoclinic bifurcation creates or destroys a single closed orbit. However, when the dimension of the system is greater than 2, it is well known that the appearance of a homoclinic orbit associated to a hyperbolic equilibrium may give rise to a richness of periodic and aperiodic motions. A review of results on the dynamical consequences of some homoclinic and heteroclinic motions in two, three and four dimensions is described by Wiggins [41].

This subsection summarizes some well-known results about the dynamics near homoclinic orbits associated to a hyperbolic equilibrium p_0 in a three-dimensional manifold. All results will be applied in the present work. We are assuming that $\dim W^s(p_0) = 2 = \dim W^u(p_0) + 1$. For more details, see the books Shilnikov *et al* [39, 40].

In three-dimensional flows, if p_0 is a saddle-focus of (2.2) such that:

- the eigenvalues of df, at p_0, are $\lambda^s + i\omega$ and λ^u, where $-\lambda^s \neq \lambda^u$ are positive numbers and $\omega \neq 0$;
- (non-linear condition) there is a homoclinic trajectory Γ connecting p_0 to itself,

then Γ is said a *Shilnikov homoclinic connection* of p_0. It is easy to see that p_0 possesses a local two-dimensional stable manifold and a local one-dimensional unstable manifold which intersect non-transversely. If $-\lambda^s < \lambda^u$, we say that the homoclinic orbit Γ satisfies the *Shilnikov condition* (see Gaspard [17]). Let Γ be a Shilnikov homoclinic connection to an equilibrium p_0 of the flow of (2.2).

1. If Γ *satisfies the Shilnikov condition,* then there exists a countable infinity of suspended Smale horseshoes (accumulating on the homoclinic cycle) in any small cylindrical neighbourhood of Γ. When the vector field is perturbed to break the homoclinic connection, finitely many of these horseshoes remain and there appear persistent strange attractors [34]. For each $N \in \mathbf{N}$, N–homoclinic orbits exist for infinitely many parameter values.
2. If Γ *does not satisfy the Shilnikov condition*, then the homoclinic orbit is an attractor. Under small C^1– perturbations, there is one stable periodic orbit in a neighbourhood of the homoclinic orbit.

In both cases, we assume that $-\lambda^s \neq \lambda^u$. Reverting the time, dual results may be obtained for homoclinic orbits involving a saddle-focus p_0 such that $\dim W^u(p_0) = 2 = \dim W^s(p_0) + 1$.

2.5.2 Homoclinic orbits near the ghost of the network

In general, the existence of a homoclinic orbit is not a robust property. Here, we prove that the homoclinic orbits of $\mathbf{v}$ and $\mathbf{w}$ occur along lines in the two parameter space (λ_1, λ_2). There are two main theorems in this section: the first one characterizes the dynamics near the homoclinic orbits associated to $\mathbf{v}$ and the other states the similar results for $\mathbf{w}$. Both follow from the analysis of the bifurcation diagram depicted in figure 6.

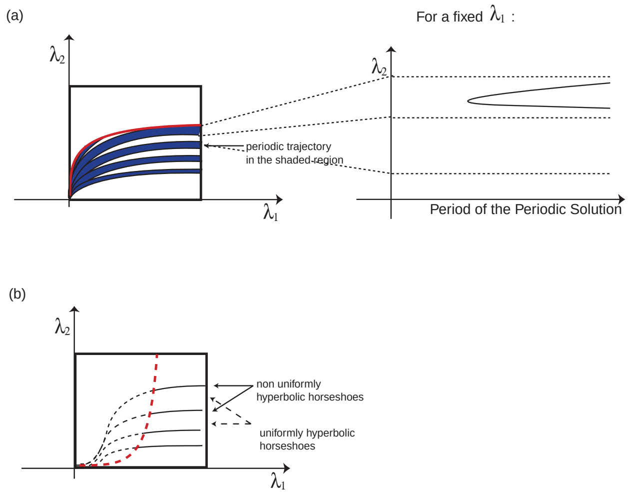

Figure 6: Bifurcation diagrams. (a) In the bifurcation diagram (λ_1, λ_2), there are infinitely many tongues of attracting periodic trajectories accumulating on the line $\lambda_2 = 0$. These periodic trajectories are bifurcating from the attracting homoclinic orbit of $\mathbf{v}$; (b) In the bifurcation diagram (λ_1, λ_2), near each homoclinic orbit of $\mathbf{w}$, there are infinitely many non-uniformly hyperbolic horseshoes which are destroyed under small perturbations. The curves for which we observe the existence homoclinic orbits of $\mathbf{w}$ are accumulating on the line $\lambda_2 = 0$.

Theorem 7 *Consider a vector field f_0 satisfying (P1)–(P4) and (P8). A generic symmetry-breaking family $f(x, \lambda_1, \lambda_2)$ unfolding f_0 satisfies (P5)–(P7) and its dynamics, for $\lambda_1 \neq 0$ and for $\lambda_2 \neq 0$ sufficiently small satisfies:*

1. *for each $\lambda_1 > 0$, there exists a sequence of positive numbers $\lambda_2^k(\mathbf{v})$ such that if $\lambda_2 = \lambda_2^k(\mathbf{v})$ there exists an attracting homoclinic orbit associated to $\mathbf{v}$;*

2. *the homoclinic orbits which exist for $\lambda_2 = \lambda_2^k(\mathbf{v})$ and for $\lambda_2 = \lambda_2^{k+2}(\mathbf{v})$ are distinguished by the number of revolutions inside W around $W^s_{loc}(\mathbf{w})$;*

3. *for each $\lambda_1 > 0$, either for $\lambda_2^k(\mathbf{v}) < \lambda_2 < \lambda_2^{k+1}(\mathbf{v})$ or for $\lambda_2^{k+1}(\mathbf{v}) < \lambda_2 < \lambda_2^{k+2}(\mathbf{v})$, there exists an attracting periodic solution near the locus of the homoclinic orbit;*

4. *in the bifurcation diagram, the tongues for which there are no attracting limit cycles (associated to bifurcations of homoclinic orbits of $\mathbf{v}$) are alternated;*

5. *when $\lambda_2 \to 0$, the homoclinic orbits of $\mathbf{v}$ accumulate on the heteroclinic connection $[\mathbf{v} \to \mathbf{w}]$.*

Note that $\lambda_2^k(\mathbf{v})$ depends on λ_1. We omit this dependence to simplify the notation. From a simple analysis of the bifurcation diagram, it follows that along a vertical line $(\lambda_1 = \lambda_1^0)$, a stable limit cycle is born from a simple homoclinic loop for $\lambda_2 = \lambda_2^k(\lambda_1^0)$; along the path, the limit cycle decreases its period and increases once again until it reaches $\lambda_2 = \lambda_2^{k+1}(\lambda_1^0)$ where the stable periodic solution becomes once again a homoclinic orbit of $\mathbf{v}$.

We have the following result concerning homoclinicities of $\mathbf{w}$:

Theorem 8 *Consider a vector field f_0 satisfying (P1)–(P4) and (P8). A generic symmetry-breaking family $f(x, \lambda_1, \lambda_2)$ unfolding f_0 satisfies (P5)–(P7) and its dynamics, for $\lambda_1 \neq 0$ and for $\lambda_2 \neq 0$ sufficiently small satisfies:*

1. *for each $\lambda_1 > 0$, there exists a sequence of positive numbers $\lambda_2^k, (\mathbf{w})$ such that if $\lambda_2 = \lambda_2^k(\mathbf{w})$ there exists a homoclinic orbit associated to $\mathbf{w}$;*
2. *the homoclinic orbits which exist for $\lambda_2 = \lambda_2^k(\mathbf{w})$ and for $\lambda_2 = \lambda_2^{k+2}(\mathbf{w})$ are distinguished by the number of revolutions inside V around $W^u_{loc}(\mathbf{v})$;*
3. *if $\lambda_2 = \lambda_2^k(\mathbf{w})$ there exists a horseshoe with an infinite number of periodic orbits;*
4. *when $\lambda_2 \to 0$, the sequence of homoclinic orbits of $\mathbf{w}$ accumulates on the cycle.*

In the bifurcation diagram of figure 6, when we follow along a vertical line ($\lambda_1 = \lambda_1^0$), we observe period-doubling cascade bifurcations that destabilize and restabilize the periodic orbits leading to the full horseshoe which exists near the homoclinic orbit of $\mathbf{w}$ – see Glendinning and Sparrow [19], Yorke and Alligood [43]. In [19], it has been demonstrated the existence of a sequence of real numbers s_i, such that for $\lambda_2 = s_i$ one observe a double pulse homoclinic orbit exhibiting the same behaviour as the main homoclinic orbit. This double pulse follows the primary homoclinic cycle twice. The existence of n–pulse homoclinic orbits ($n > 2$) has been also showed.

For dissipative systems, the process of creation and destruction of horseshoes can be accompanied by unfoldings of homoclinic tangencies to hyperbolic periodic solutions. The co-existence of different types of behaviour in the flow has been investigated by many authors – see Bykov [9], Xiao-Feng and Rui-hai [42], Glendinning, Abshagen and Mullin [18]. In the present paper, from the analysis of the bifurcation diagrams, we may conclude that:

Corollary 9 *For any family of differential equations satisfying (P1)–(P5) and (P8) the co-existence of the homoclinic trajectories of $\mathbf{v}$ and $\mathbf{w}$ is a codimension 2 phenomenon.* [2].

Note that the coexistence of homoclinic trajectories is not a *true* bifurcation since these trajectories occur in different regions of the phase space. Due to the property (P8), the homoclinic trajectories associated to $\mathbf{v}$ and $\mathbf{w}$, when both coexist, must be linked; each one winds around the other infinitely many times, inside the linearized neighbourhood defined in section 3.

3 Local Dynamics near the saddles

In this section, we establish local coordinates near the saddle-foci $\mathbf{v}$ and $\mathbf{w}$ and define some notation that will be used in the rest of the paper. The starting point is an application of Samovol's Theorem [37] to linearize the flow around the equilibria and to introduce cylindrical coordinates around each saddle-focus. These are used to define neighbourhoods with boundary transverse to the linearized flow. For each saddle, we obtain the expression of the local map that sends points in the boundary where the flow goes in, into points in the boundary where the flows goes out. Finally, we establish a convention for the transition maps from one neighbourhood to the other.

Note that when we refer to the stable/unstable manifold of an equilibrium point, we mean the *local* stable/unstable manifold of that equilibrium.

[2]They occur at isolated points in parameter space, accumulating at the origin.

3.1 Linearization near the equilibria

By Samovol's Theorem [37] (see also section 6.4 Part I of Anosov *et al* [7] and Ren & Yang [35]), around the saddle-foci, the vector field f is C^1-conjugated to its linear part, since there are no resonances of order 1. In cylindrical coordinates (ρ, θ, z) the linearizations at $\mathbf{v}$ and $\mathbf{w}$ take the form, respectively:

$$\begin{cases} \dot{\rho} = -C_{\mathbf{v}}\rho \\ \dot{\theta} = \alpha_{\mathbf{v}} \\ \dot{z} = E_{\mathbf{v}} z \end{cases} \qquad \begin{cases} \dot{\rho} = E_{\mathbf{w}}\rho \\ \dot{\theta} = \alpha_{\mathbf{w}} \\ \dot{z} = -C_{\mathbf{w}} z. \end{cases} \tag{3.3}$$

We consider cylindrical neighbourhoods of $\mathbf{v}$ and $\mathbf{w}$ in $\mathbf{S}^3$ of radius $\varepsilon > 0$ and height 2ε that we denote by V and W, respectively. Their boundaries consist of three components (see figure 7):

- The cylinder wall parametrized by $x \in \mathbf{R}$ (mod 2π) and $|y| \leq \varepsilon$ with the usual cover $(x, y) \mapsto (\varepsilon, x, y) = (\rho, \theta, z)$. Here x represents the angular coordinate and y is the height of the cylinder.

- Two disks, the top and the bottom of the cylinder. We take polar coverings of these disks: $(r, \varphi) \mapsto (r, \varphi, j\varepsilon) = (\rho, \theta, z)$ where $j \in \{-, +\}$, $0 \leq r \leq \varepsilon$ and $\varphi \in \mathbf{R}$ (mod 2π).

On these cross sections, we define the return maps to study the dynamics near the cycle.

Remark 1 *Property (P8) concerning the direction of turning around the connection* $[\mathbf{v} \to \mathbf{w}]$*, may be interpreted in terms of the sign of* $\alpha_{\mathbf{v}}$ *and* $\alpha_{\mathbf{w}}$*: property (P8) holds when they have the same signs.*

3.2 Coordinates near v

The cylinder wall is denoted by $H^{in}_{\mathbf{v}}$. Trajectories starting at interior points of $H^{in}_{\mathbf{v}}$ go into V in positive time and $H^{in}_{\mathbf{v}} \cap W^s(\mathbf{v})$ is parametrized by $y = 0$. The set of points in $H^{in}_{\mathbf{v}}$ with positive (resp. negative) second coordinate is denoted by $H^{in,+}_{\mathbf{v}}$ (resp. $H^{in,-}_{\mathbf{v}}$).

The top and the bottom of the cylinder are denoted, respectively, $H^{out,+}_{\mathbf{v}}$ and $H^{out,-}_{\mathbf{v}}$. Trajectories starting at interior points of $H^{out,+}_{\mathbf{v}}$ and $H^{out,-}_{\mathbf{v}}$ go inside the cylinder in negative time.

After linearization $W^u(\mathbf{v})$ is the z-axis, intersecting $H^{out,+}_{\mathbf{v}}$ at the origin of coordinates of $H^{out,+}_{\mathbf{v}}$. Trajectories starting at $H^{in,j}_{\mathbf{v}}$, $j \in \{+, -\}$ leave V at $H^{out,j}_{\mathbf{v}}$.

3.3 Coordinates near w

After linearization, $W^s(\mathbf{w})$ is the z -axis, intersecting the top and bottom of the cylinder at the origin of its coordinates. We denote by $H^{in,j}_{\mathbf{w}}$, $j \in \{-, +\}$, its two components. Trajectories starting at interior points of $H^{in,\pm}_{\mathbf{w}}$ go into W in positive time.

Trajectories starting at interior points of the cylinder wall $H^{out}_{\mathbf{w}}$ go into W in negative time. The set of points in $H^{out}_{\mathbf{w}}$ whose second coordinate is positive (resp. negative) is denoted $H^{out,+}_{\mathbf{w}}$ (resp. $H^{out,-}_{\mathbf{w}}$) and $H^{out}_{\mathbf{w}} \cap W^u(\mathbf{w})$ is parametrized by $y = 0$. Trajectories that start at $H^{in,j}_{\mathbf{w}} \backslash W^s(\mathbf{w})$, $j \in \{+, -\}$ leave the cylindrical neighbourhood at $H^{out,j}_{\mathbf{w}}$.

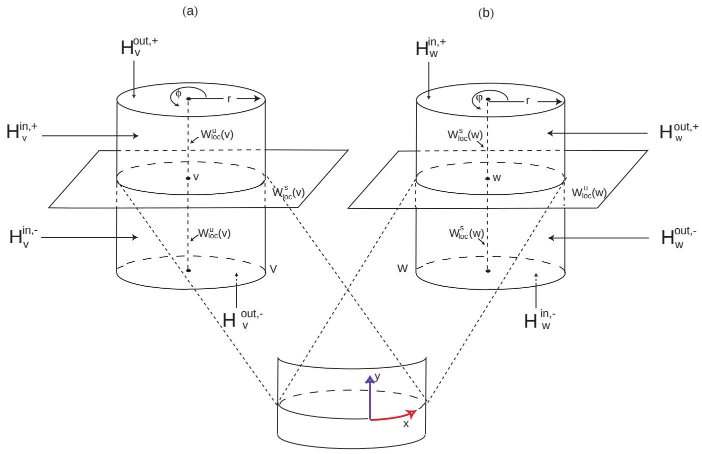

Figure 7: Neighbourhoods of the saddle-foci. (a) Once the flow goes in the cylinder V transversely across the wall $H_{\mathbf{v}}^{in} \backslash W^s(\mathbf{v})$, it leaves transversely across the top or the bottom $H_{\mathbf{v}}^{out}$; (b) Once the flow goes in the cylinder $\mathbf{w}$ transversely across the top or the bottom $H_{\mathbf{w}}^{in} \backslash W^s(\mathbf{w})$, it leaves transversely across the wall $H_{\mathbf{w}}^{out}$. Inside both cylinders, the vector field is linearized.

3.4 Local map near v

The local map $\Phi_{\mathbf{v}} : H_{\mathbf{v}}^{in,+} \to H_{\mathbf{v}}^{out,+}$ near $\mathbf{v}$ is given by

$$\Phi_{\mathbf{v}}(x, y) = (c_1 y^{\delta_{\mathbf{v}}}, -g_{\mathbf{v}} \ln y + x + c_2) = (r, \phi) \tag{3.4}$$

where $\delta_{\mathbf{v}}$ is the saddle index of $\mathbf{v}$,

$$\delta_{\mathbf{v}} = \frac{C_{\mathbf{v}}}{E_{\mathbf{v}}} > 1, \quad c_1 = \varepsilon^{1-\delta_{\mathbf{v}}} > 0, \quad g_{\mathbf{v}} = \frac{\alpha_{\mathbf{v}}}{E_{\mathbf{v}}} \quad \text{and} \quad c_2 = g_{\mathbf{v}} \ln(\varepsilon).$$

The expression for the local map from $H_{\mathbf{v}}^{in,-}$ to $H_{\mathbf{v}}^{out,-}$ we obtain for $y < 0$, $\phi_{\mathbf{v}}(x, y) = \phi_{\mathbf{v}}(x, -y)$.

3.5 Local map near w

The local map $\Phi_{\mathbf{w}} : H_{\mathbf{w}}^{in,+} \backslash W^s(\mathbf{w}) \to H_{\mathbf{w}}^{out,+}$ near $\mathbf{w}$ is given by:

$$\Phi_{\mathbf{w}}(r, \varphi) = (c_3 - g_{\mathbf{w}} \ln r + \varphi, c_4 r^{\delta_{\mathbf{w}}}) = (x, y) \ ,$$

where $\delta_{\mathbf{w}}$ is the saddle index of $\mathbf{w}$,

$$\delta_{\mathbf{w}} = \frac{C_{\mathbf{w}}}{E_{\mathbf{w}}} > 1, \quad g_{\mathbf{w}} = \frac{\alpha_{\mathbf{w}}}{E_{\mathbf{w}}}, \quad c_3 = g_{\mathbf{w}} \ln \varepsilon \quad \text{and} \quad c_4 = \varepsilon^{1-\delta_{\mathbf{w}}} > 0.$$

The same expression holds for the local map from $H_{\mathbf{w}}^{in,-} \backslash W^s(\mathbf{w})$ to $H_{\mathbf{w}}^{out,-}$.

3.6 Geometry near the saddle-foci v and w

The notation and constructions of previous subsections are now used to study the geometry associated to the local dynamics around each saddle-focus.

Definition 1 *1. A* segment β on *$H_{\mathbf{v}}^{in}$ or $H_{\mathbf{w}}^{out}$ is a smooth regular parametrized curve of the type $\beta : [0,1] \to H_{\mathbf{v}}^{in}$ or $\beta : [0,1] \to H_{\mathbf{w}}^{out}$ that meets $W_{loc}^s(\mathbf{v})$ or $W_{loc}^u(\mathbf{w})$ transversely at the point $\beta(1)$ only and such that, writing $\beta(s) = (x(s), y(s))$, both x and y are monotonic functions of s.*

2. A spiral on *$H_{\mathbf{v}}^{out}$ or $H_{\mathbf{w}}^{in}$* around *a point p is a curve $\alpha : [0,1) \to H_{\mathbf{v}}^{out}$ or $\alpha : [0,1) \to H_{\mathbf{w}}^{in}$ satisfying $\lim_{s \to 1^-} \alpha(s) = p$ and such that, if $\alpha(s) = (\alpha_1(s), \alpha_2(s))$ are its expressions in polar coordinates (ρ, θ) around p, then α_1 and α_2 are monotonic, with $\lim_{s\to 1^-} |\alpha_2(s)| = +\infty$.*

3. Let $a, b \in \mathbf{R}$ such that $a < b$ and let $H_{\mathbf{w}}^{out}$ be a surface parametrized by a covering $(\theta, h) \in \mathbf{R} \times [a, b]$ where θ is periodic. A helix on $H_{\mathbf{w}}^{out}$ accumulating on the circle $h = h_0$ *is a curve $\gamma : [0,1) \to H$ such that its coordinates $(\theta(s), h(s))$ are monotonic functions of s with $\lim_{s\to 1^-} h(s) = h_0$ and $\lim_{s\to 1^-} |\theta(s)| = +\infty$.*

At the item 2 of the previous definition, p will be seen as the intersection of the one-dimensional local stable/unstable manifold of $\mathbf{v}$ or $\mathbf{w}$ with the considered cross section. At the item 3, the curve is the intersection of the two-dimensional local unstable manifold of $\mathbf{w}$ with the cross section $H_{\mathbf{w}}^{out}$. Observing figure 8, the definitions become clear. The next lemma summarizes some basic technical results about the geometry near the saddle-foci. The proof may be found in section 6 of Aguiar *et al* [5] - this is why it will be omitted here.

Lemma 10 *1. For $j \in \{+, -\}$, a segment β on $H_{\mathbf{v}}^{in,j}$ is mapped by $\phi_{\mathbf{v}}$ into a spiral on $H_{\mathbf{v}}^{out,j}$ around $W^u(\mathbf{v})$;*

2. For $j \in \{+, -\}$, a segment β on $H_{\mathbf{w}}^{out,j}$ is mapped by $\phi_{\mathbf{w}}^{-1}$ into a spiral on $H_{\mathbf{w}}^{in,j}$ around $W^s(\mathbf{w})$;

3. For $j \in \{+, -\}$, a spiral on $H_{\mathbf{w}}^{in,j}$ around $W^s(\mathbf{w})$ is mapped by $\phi_{\mathbf{w}}$ into a helix on $H_{\mathbf{w}}^{out,j}$ accumulating on the circle $H_{\mathbf{w}}^{out} \cap W^u(\mathbf{w})$.

On the proof of item 3 of lemma 10, the authors of [5] used implicitly that *the orientations in which trajectories turn around in V and W are the same* (i.e., they used implicitly property (P8)).

3.7 Transition Maps

In the rest of this paper, we study the Poincaré first return map on the boundaries defined in this section. Consider the transition maps

$$\Psi_{\mathbf{v},\mathbf{w}} : H_{\mathbf{v}}^{out,j} \longrightarrow H_{\mathbf{w}}^{in,j} \qquad j = +, - \quad \text{and} \quad \Psi_{\mathbf{w},\mathbf{v}} : H_{\mathbf{w}}^{out} \longrightarrow H_{\mathbf{v}}^{in}.$$

For $\lambda_1 = 0$, the map $\Psi_{\mathbf{w},\mathbf{v}}$ may be taken to be the identity. For $\lambda_1 \neq 0$, the map can be seen as a rotation by an angle $\alpha(\lambda_1)$ with $\alpha(0) = 0$. Without loss of generality, we use $\alpha \equiv \frac{\pi}{2}$, that simplifies the expressions used.

For $\lambda_2 = 0$ one of the connections $[\mathbf{v} \to \mathbf{w}]$ goes from $H_{\mathbf{v}}^{out,+}$ to $H_{\mathbf{w}}^{in,+}$. For $\lambda_2 = 0$, the linear part of the map $\Psi_{\mathbf{v},\mathbf{w}}$ may be represented (in rectangular coordinates) as the composition of a rotation of the coordinate axes and a change of scales. As in Bykov [9], after a rotation and a uniform rescaling of the coordinates, we may assume without loss of generality that for $\lambda_2 \neq 0$, $\Psi_{\mathbf{v},\mathbf{w}}$ is given by the map $T(x, y) + L(x, y)$, where:

$$T(x,y) = \begin{pmatrix} \lambda_2 \\ 0 \end{pmatrix} \qquad \text{and} \qquad L(x,y) = \begin{pmatrix} a & 0 \\ 0 & \frac{1}{a} \end{pmatrix} \qquad a \in \mathbf{R}^+ \backslash \{1\}.$$

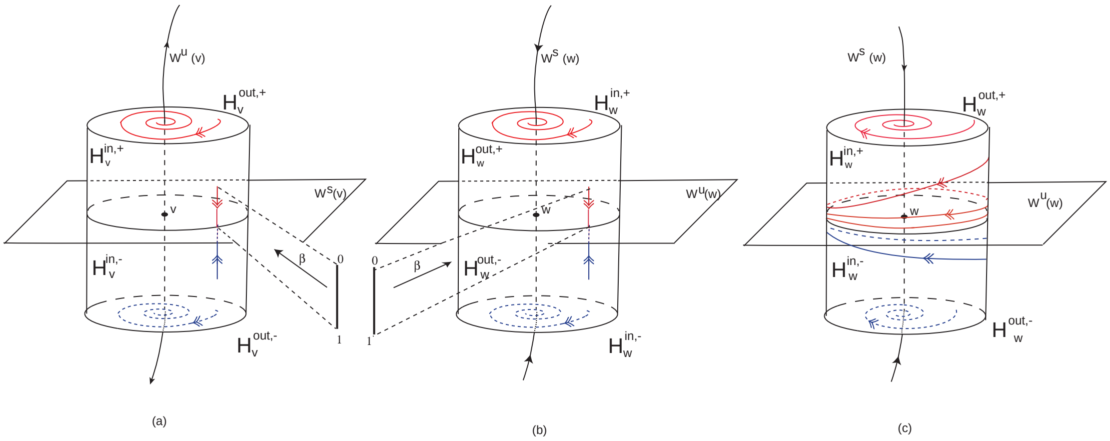

Figure 8: Smooth structures referred in lemma 10. (a) A segment β on $H_{\mathbf{v}}^{in,j}$ is mapped by $\phi_{\mathbf{v}}$ into a spiral on $H_{\mathbf{v}}^{out,j}$ around $W^u(\mathbf{v})$. (b) A segment β on $H_{\mathbf{w}}^{out,j}$ is mapped by $\phi_{\mathbf{w}}^{-1}$ into a spiral on $H_{\mathbf{w}}^{in,j}$ around $W^s(\mathbf{w})$. (c) A spiral on $H_{\mathbf{w}}^{in,j}$ around $W^s(\mathbf{w})$ is mapped by ϕ_w into a helix on $H_{\mathbf{w}}^{out,j}$ accumulating on the circle $H_{\mathbf{w}}^{out} \cap W^u(\mathbf{w})$. The double arrows on the segments, spiral and helix indicate correspondence of orientation and not the flow.

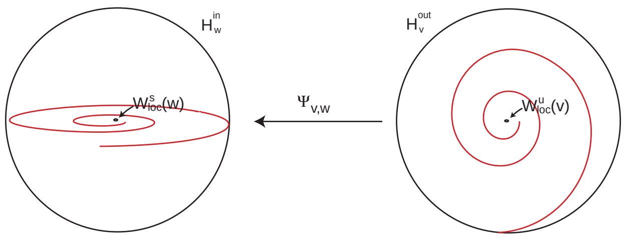

Figure 9: The transition map from $\mathbf{v}$ to $\mathbf{w}$. We set that the transition map from $\mathbf{v}$ to $\mathbf{w}$ may be approximated by a diagonal map.

Note that the map $\Psi_{\mathbf{v},\mathbf{w}}$ is given in rectangular coordinates. To compose this map with $\Phi_{\mathbf{w}}$, it is required to change the coordinates. We address this issue later in section 5. We summarize the above information in Table 3.

Parameters	Symmetries preserved	$\Psi_{\mathbf{v},\mathbf{w}}$	$\Psi_{\mathbf{w},\mathbf{v}}$
$\lambda_1 = \lambda_2 = 0$	γ_1, γ_2	L	Identity
$\lambda_1 \neq 0$ and $\lambda_2 = 0$	γ_1	L	Rotation
$\lambda_1 = 0$ and $\lambda_2 \neq 0$	γ_2	$T \circ L$	Identity
$\lambda_1 \neq 0$ and $\lambda_2 \neq 0$	Identity	$T \circ L$	Rotation

Table 3: The transition maps $\Psi_{\mathbf{v},\mathbf{w}}$ and $\Psi_{\mathbf{w},\mathbf{v}}$ depend on the type of symmetry breaking.

With this choice of local coordinates the maps $\Psi_{\mathbf{v}}$ and $\Psi_{\mathbf{w}}$ do not depend on λ_1, λ_2. The transition map $\Psi_{\mathbf{w},\mathbf{v}}$ may be taken to depend on λ_1 but not on λ_2 and is written as $\Psi_{\mathbf{w},\mathbf{v}}(x, y, \lambda_1)$. The other transition map $\Psi_{\mathbf{v},\mathbf{w}}$ may be taken to depend on λ_2 but not on λ_1 and is written as $\Psi_{\mathbf{v},\mathbf{w}}(r, \varphi, \lambda_2)$ (see figure 9).

4 Transverse Intersection of 2-dimensional manifolds

In this section, when we break the $\mathbf{Z}_2(\gamma_2)$ equivariance, using property (P6), we are assuming that the heteroclinic connection between $\mathbf{w}$ and $\mathbf{v}$ becomes transverse and one-dimensional. We still have a heteroclinic network of a different nature, which will be denoted by $\Sigma^\star$.

4.1 Proof of Proposition 2

Items 1 and 2 of proposition 2 follow from the three facts:

- the equilibria are hyperbolic;
- the fixed point subspace that contains the two connections $[\mathbf{v} \to \mathbf{w}]$ remains invariant;
- $\dim W^u(\mathbf{v}) \cap W^s(\mathbf{w}) = 1$ and $W^u(\mathbf{v}) \cap W^s(\mathbf{w}) \subset Fix\,\langle\gamma_1\rangle$.

Item 3 is a direct consequence of the main result about finite and infinite switching of Aguiar *et al* [5]. Item 4 follows straightforwardly from the referred paper picking the segment β as $W^u(\mathbf{w}) \cap H^{in}_{\mathbf{v}}$.

In order to prove item 5, we start with some terminology about horizontal and vertical strips. Given a rectangular region $\mathcal{R}$ in $H^{in}_{\mathbf{v}}$ or in $H^{out}_{\mathbf{w}}$ parametrized by a rectangle $R = [w_1, w_2]\times[z_1, z_2]$, a *horizontal strip* in $\mathcal{R}$ will be parametrized by:

$$\mathcal{H} = \{(x, y) : x \in [w_1, w_2], y \in [u_1(x), u_2(x)]\},$$

where

$$u_1, u_2 : [w_1, w_2] \to [z_1, z_2]$$

are Lipschitz functions such that $u_1(x) < u_2(x)$. The *horizontal boundaries* of the strip are the lines parametrized by the graphs of the u_i, the *vertical boundaries* are the lines $\{w_i\} \times [u_1(w_i), u_2(w_i)]$ and its *heigth* is

$$h = \max_{x\in[w_1,w_2]} (u_2(x) - u_1(x))\,.$$

When both $u_1(x)$ and $u_2(x)$ are constant functions we call $\mathcal{H}$ a *horizontal rectangle across* $\mathcal{R}$. A *vertical strip across* $\mathcal{R}$, its *width* and a *vertical rectangle* have similar definitions, with the roles of x and y reversed.

Item 5 follows from the construction of the Cantor sets presented in Aguiar *et al* [3] – if $R_{\mathbf{v}} \subset H^{in}_{\mathbf{v}}$ is a rectangle containing $[\mathbf{w} \to \mathbf{v}] \cap H^{in}_{\mathbf{v}}$ on its border, the initial conditions that returns to $H^{in}_{\mathbf{v}}$ are contained in a sequence of horizontal strips accumulating on the stable manifold of $\mathbf{v}$, whose heights tend to zero. Each one of these horizontal strips lying on the rectangle $R_{\mathbf{v}} \subset H^{in}_{\mathbf{v}}$, is mapped by $\Phi_{\mathbf{w}} \circ \Psi_{\mathbf{v},\mathbf{w}} \circ \Phi_{\mathbf{v}}$ into a horizontal strip across $H^{out}_{\mathbf{w}}$. By (P6), they are mapped by $\Psi_{\mathbf{v},\mathbf{w}}$ into vertical strips across $R_{\mathbf{w}}$ crossing transversely the original. This gives rise to a nested chain of uniformly hyperbolic horseshoes, accumulating on the heteroclinic connection, each one with positive topological entropy [16]. The hyperbolicity guarantees that these invariant sets persist under symmetry breaking perturbations. An illustration of the way these horseshoes are appearing is given in figure 5. However, note that among the infinitely many nested horseshoes that occur when there is a heteroclinic network, only finitely many persist under generic C^1–perturbations.

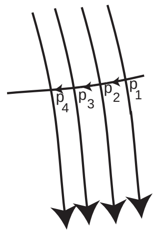

Figure 10: Pleated diagram associated to G_n, the spine of the generalized horseshoe: given two oriented horizontal and vertical boundaries in $R_{\mathbf{v}}$, h and v respectively, the pleated diagram associated to the horseshoe is the union of the oriented arcs $h \cup \Psi_{\mathbf{w},\mathbf{v}} \circ \Phi_{\mathbf{w}} \circ \Psi_{\mathbf{v},\mathbf{w}} \circ \Phi_{\mathbf{v}}(v)$ (adapted definition of Hirasawa and Kin [22]).

4.2 Proof of Corollary 5

The proof of Corollary 5 is connected with the geometry of the horseshoe G_n (with n strips) which arises near the cycle (see item 5 of proposition 2). Each horizontal strip in $H_{\mathbf{v}}^{in}$ is mapped by the first return map into a vertical strip. This vertical strip intersects transversely n times the original horizontal strip. As in Hirasawa *et al* [22], denoting the consecutive intersection points by $p_1, \ldots, p_n$, we are able to construct the *twist signature* of the horseshoe associated to G_n: it is a finite sequence of integers $(a_i)_{i \in \{1,\ldots,n\}}$ satisfying the following conditions:

- $a_1 = 0$;
- $a_i = a_{i-1} + 1$ if the oriented segment $[p_{i-1}, p_i]$ goes around the counterclockwise direction;
- $a_i = a_{i-1} - 1$ if the oriented segment $[p_{i-1}, p_i]$ goes around the clockwise direction.

We will use the following result of Hirasawa and Kin [22] [adapted]:

Theorem 11 *Let G a generalized horseshoe map with twist signature $(a_1, a_2, \ldots, a_n)$. Then G induces all link types if and only if one of the following is satisfied:*

- *each $a_i \geq 0$ and $\max\{a_i\} \geq 3$.*
- *each $a_i \leq 0$ and $\max\{a_i\} \geq -3$.*

For $n > 2$, the generalized horseshoe G_n induces all links because the admissible signatures are of the type $(0, 1, 2, 3, \ldots, n)$ or $(0, -1, -2, -3, \ldots, -n)$ – the intersection of the horseshoes is clear in the arrows in figure 10.

5 Proof of Theorem 6: existence of periodic trajectories

In this section, we treat the case $\lambda_1 = 0$ and $\lambda_2 \neq 0$, when the two-dimensional manifolds $W^u(\mathbf{w})$ and $W^s(\mathbf{v})$ coincide. We prove theorem 6 – the existence of a non-trivial closed trajectory – by finding a fixed point of the Poincaré first return map R in $H_{\mathbf{w}}^{in}$.

5.1 Poincaré Map

Since $\lambda_1 = 0$, then $\Psi_{\mathbf{w},\mathbf{v}}$ is the identity. The symmetry γ_2 is preserved and thus the two half-spheres in $\mathbf{S}^3 \backslash Fix(\langle \gamma_2 \rangle)$ are flow-invariant with symmetric dynamics. We look at one of them, where for $\lambda_2 = 0$ the connection goes from $H_{\mathbf{v}}^{out,+}$ to $H_{\mathbf{w}}^{in,+}$, omitting the redundant + signs to lighten the notation. Consider the map:

$$R_* = \Phi_{\mathbf{v}} \circ \Psi_{\mathbf{w},\mathbf{v}} \circ \Phi_{\mathbf{w}} : H_{\mathbf{w}}^{in} \backslash W_{loc}^u(\mathbf{w}) \quad \longrightarrow \quad H_{\mathbf{v}}^{out}$$

that in polar coordinates is given by

$$R_*(r,\varphi) = \Big(c_5 r^{\delta}, c_6 + \varphi - c_7 \ln(r)\Big) = (\rho, \theta) \tag{5.5}$$

where

$$c_5 = c_1 c_4^{\delta_{\mathbf{v}}} = \varepsilon^{1-\delta}, \quad \delta = \delta_{\mathbf{v}}\delta_{\mathbf{w}} \quad c_6 = -g_{\mathbf{v}} \ln(c_4) + c_2 + c_3 \quad c_7 = g_{\mathbf{v}}\delta_{\mathbf{w}} + g_{\mathbf{w}}$$

and, due to (P2), we have:

$$\delta = \delta_{\mathbf{v}}\delta_{\mathbf{w}} = \frac{C_{\mathbf{v}} C_{\mathbf{w}}}{E_{\mathbf{v}} E_{\mathbf{w}}} > 1. \tag{5.6}$$

It is worth noting that:

$$c_7 = g_{\mathbf{v}}\delta_{\mathbf{w}} + g_{\mathbf{w}} > 0.$$

In Cartesian coordinates, we have $R_*(r,\varphi) = (\rho\cos\theta, \rho\sin\theta) = (x,y)$. The Poincaré first return map is λ_2–dependent and given by $R(r,\varphi) = \Psi_{\mathbf{w},\mathbf{v}}(R_*(r,\varphi), \lambda_2)$, where $\Psi_{\mathbf{w},\mathbf{v}} : H_{\mathbf{v}}^{out} \longrightarrow H_{\mathbf{w}}^{in}$ is given by $\Psi_{\mathbf{w},\mathbf{v}}(x,y) = (x + \lambda_2, y)$.

5.2 There are no multi-pulse heteroclinic connections $[\mathbf{v} \to \mathbf{w}]$

In this section, we will prove the first assertion of theorem 6. Reminding that V and W are neighbourhoods of $\mathbf{v}$ and $\mathbf{w}$ in which the vector field can be C^1–linearized, we start by making the statement of theorem 6 more precise:

Definition 2 *Let $A \subset V$ be a cross-section to the flow meeting $W^u(\mathbf{v})$. A one-dimensional connection $[\mathbf{v} \to \mathbf{w}]$ that meets A at precisely k points is called a k–*pulse heteroclinic connection with respect to A. *If $k > 1$ we call it a multi-pulse heteroclinic connection. A similar definition holds for a cross-section $B \subset W$ and for pairs of cross-sections A, B.*

We intend to show that generically in a one-parameter unfolding satisfying (P1)–(P5) and (P7), with $\lambda_1 = 0$, there are no multi-pulse heteroclinic connections with respect to $A = H_{\mathbf{v}}^{out}$. Then a 2–pulse heteroclinic connection occurs for $\lambda_2 = \lambda_*$ whenever R maps $\Psi_{\mathbf{v},\mathbf{w}}(0,0,\lambda_*) \in H_{\mathbf{w}}^{in}$ into the origin of $H_{\mathbf{w}}^{out}$. A k–pulse connection arises when $R^k\left(\Psi_{\mathbf{v},\mathbf{w}}(0,0,\lambda_*)\right) = (0,0)$ and $R^j\left(\Psi_{\mathbf{v},\mathbf{w}}(0,0,\lambda_*)\right) \neq (0,0)$ for $0 < j < k$. Thus, in order to find a value λ_* where there is a multi-pulse connection one has to solve the two equations $R^k\left(\Psi_{\mathbf{v},\mathbf{w}}(0,0,\lambda_*)\right) = (0,0)$ for λ_*. Generically the two equations do not have a common solution.

Remark 2 *Note that for two-parameter families, i.e. $\lambda_2 \in \mathbf{R}^2$, generically there would be isolated values λ_k for which there would be k-pulse connections. In order to get branches of multi-pulses arbitrarily close to $\lambda_2 = 0$, one would need three parameters. This codimension 3 behaviour is beyond the scope of this paper.*

5.3 Existence of a fixed point of the Poincaré map

We start by finding the radial coordinate of the fixed point. For this we consider the maps $g^{\pm} : (0, \varepsilon) \longrightarrow \mathbf{R}$ (see figure 11)

$$g^+(r) = r + \varepsilon \left(\frac{r}{\varepsilon}\right)^{\delta} \qquad g^-(r) = r - \varepsilon \left(\frac{r}{\varepsilon}\right)^{\delta} .$$

Since $\delta > 1$ both maps are of class C^1 and

$$\frac{dg^+}{dr}(0) = \frac{dg^-}{dr}(0) = 1. \tag{5.7}$$

Lemma 12 *If C is a circle of centre $(0,0)$ and radius r_0 in $H^{in}_{\mathbf{w}}$, with $0 < r_0 < \varepsilon$, then $R(C, \lambda_2)$ is a circle of centre $(\lambda_2, 0)$ and radius $c_5 r_0^{\delta} < r_0$. Moreover:*

- *if $\lambda_2 \in (g^-(r_0), g^+(r_0))$, then $R(C, \lambda_2) \cap C$ contains exactly two points;*
- *if either $\lambda_2 = g^+(r_0)$ or $\lambda_2 = g^-(r_0)$, then $R(C, \lambda_2)$ is tangent to C and thus $R(C, \lambda_2) \cap C$ contains a single point;*
- *if λ_2 lies outside the interval $[g^-(r_0), g^+(r_0)]$, then $R(C, \lambda_2) \cap C$ is empty.*

Proof: Write C in polar coordinates as (r_0, φ), where $\varphi \in [0, 2\pi)$, $r_0 \in \mathbf{R}^+_0$ is fixed, and let $R_*(r_0, \varphi) = (\rho, \theta)$. Then $\rho = c_5 r_0^{\delta}$ is constant and $\theta = \varphi + c_6 - c_7 \ln(r_0)$ varies in an interval of length 2π. Hence, $R_*(C)$ is a circle with centre $(0,0)$ and therefore, $R(C, \lambda_2) = \Psi_{\mathbf{w},\mathbf{v}} \circ R_*(C)$ is a circle with centre $(\lambda_2, 0)$ and radius $\varepsilon \left(\frac{r_0}{\varepsilon}\right)^{\delta}$. Since $r_0 < \varepsilon$ and $\delta > 1$, then this radius is less that r_0.

For $\lambda_2 = 0$, the two circles C and $R(C, \lambda_2)$ are concentric. For a fixed $r_0 > 0$, as λ_2 increases from zero, $R(C, \lambda_2)$ moves to the right and is contained in $H^{in}_{\mathbf{w}}$ as long as $\lambda_2 \leq \varepsilon \left(1 - \left(\frac{r_0}{\varepsilon}\right)^{\delta}\right)$. As $R(C, \lambda_2)$ moves to the right it has first an internal tangency to C at $\lambda_2 = g^+(r_0)$, then the two circles meet at exactly two points and at $\lambda_2 = g^-(r_0)$ they two points come together as C and $R(C, \lambda_2)$ have an external tangency (figure 11). □

Let $a(\lambda_2)$, $b(\lambda_2)$ be the inverses of the maps $\lambda_2 = g^+(r)$ and $\lambda_2 = g^-(r)$, respectively. Since g^- has a maximum at some point $r^* \in (0, \varepsilon)$ with $g^-(r^*) = \lambda_2^*$, then $b(\lambda_2)$ is defined only for $0 < \lambda_2 < \lambda_2^*$ (see figure 11). For each $r \in (a(\lambda_2), b(\lambda_2))$, in the circle C with centre at the origin and radius r there are two points whose images by R lie in the same circle. These points $P^+(r)$ and $P^-(r)$ are symmetrically placed with respect to the line that contains the centres of C and of $R(C, \lambda_2)$. In proposition 13 we show that for at least one of these points the angular coordinate is also fixed by R and that this happens for each $\lambda_2 < \lambda_2^*$.

Proposition 13 *For any λ_2 with $0 < \lambda_2 \leq \lambda_2^*$ there is a point $P \in H^{in}_{\mathbf{w}}$ such that $R(P, \lambda_2) = P$.*

Proof: Consider a fixed $\lambda_2 \in [0, \lambda_2^*]$. For this proof, we need two systems of polar coordinates in $H^{in}_{\mathbf{w}}$: one centered at $W^s(\mathbf{w}) \cap H^{in}_{\mathbf{w}}$ (that we call S_1, coordinates (r, θ)) and the other centered at $W^u(\mathbf{v}) \cap H^{in}_{\mathbf{w}}$ (that we call S_2, coordinates (ρ, φ)). The angular component of both systems of coordinates starts at the line through the two centres; for S_1 at the half-line that contains the centre of S_2, for S_2 at the half-line that does not contain the centre of S_1 (see figure 12). Both angular coordinates φ and θ are taken in $[-\pi, \pi]$ ($\mathbf{R} \pmod{2\pi}$).

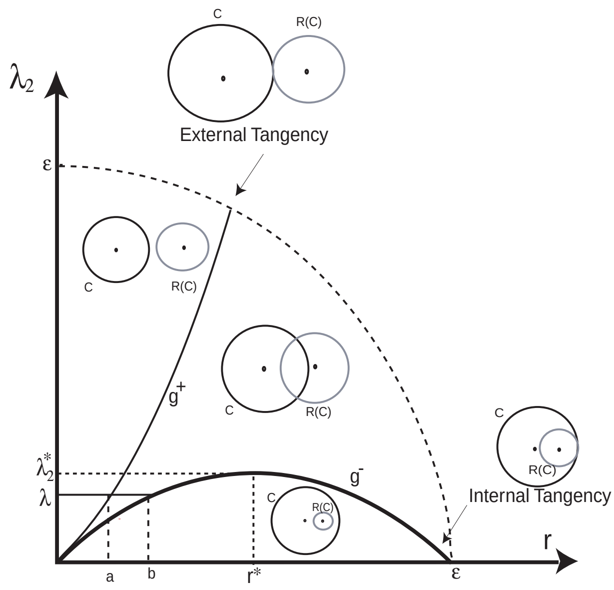

Figure 11: Thin line: graph of $g^{+}(r) = r + \varepsilon \left(\frac{r}{\varepsilon}\right)^{\delta}$ where the circle C of radius r and the circle $R(C, \lambda_2)$ have an external tangency; thick line: graph of $g^{-}(r) = r - \varepsilon \left(\frac{r}{\varepsilon}\right)^{\delta}$ where C and $R(C, \lambda_2)$ have an internal tangency. Inside the wedge-shaped region between the two curves, C meets $R(C, \lambda_2)$ at two points, outside it $C \cap R(C, \lambda_2) = \emptyset$.

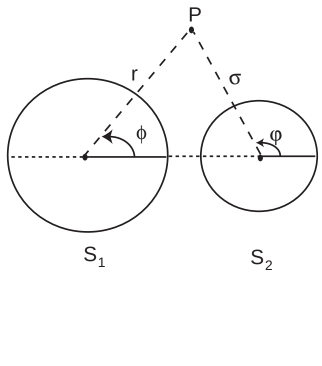

Figure 12: The two coordinate systems S_1 and S_2.

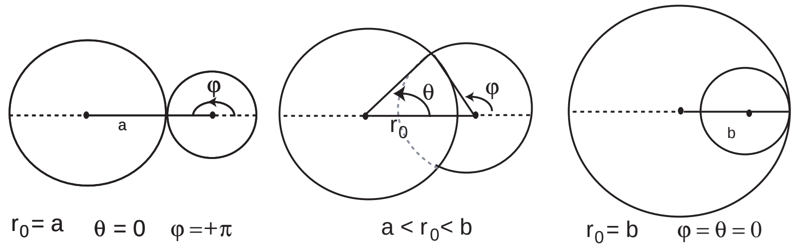

Figure 13: For a fixed $\lambda_2 < \lambda_2^*$, and for $r = a(\lambda_2) = a$, the circles C and $R(C, \lambda_2)$ have an external tangency (left). In this case, the intersection point has angular coordinate $\theta^+ = \theta^- = 0$ in S_1 and $\varphi^+ = \pi$, $\varphi^- = -\pi$ in S_2. For $r = b(\lambda_2) = b$, the circles C and $R(C, \lambda_2)$ have an internal tangency (right). Here, the intersection point has angular coordinate 0 in both coordinate systems. At the centre: for $r \in (a(\lambda_2), b(\lambda_2))$, the angular coordinate in S_2 of the upper (lower) intersection point decreases (increases) to 0 as r increases.

We begin by measuring the angular component of the two intersection points P^+ and P^- of the circles C and $R(C, \lambda_2)$. Let $\varphi^+(r)$ and $\varphi^-(r)$ stand for the angular coordinates $\varphi^+(r) = \varphi^+(P^+(r))$ and $\varphi^-(r) = \varphi^-(P^-(r))$, in the reference frame S_2 (see Figure 13). Then the functions

$$\varphi^+ : [a(\lambda_2), b(\lambda_2)] \longrightarrow [0, \pi] \qquad \varphi^- : [a(\lambda_2), b(\lambda_2)] \longrightarrow [-\pi, 0]$$

are both monotonic and satisfy

$$\varphi^+(a(\lambda_2)) = \pi \qquad \varphi^+(b(\lambda_2)) = 0 \qquad \varphi^-(a(\lambda_2)) = -\pi \qquad \varphi^-(b(\lambda_2)) = 0\ . \tag{5.8}$$

Similarly, $\theta^+(r) = \theta^+(P^+(r))$ and $\theta^-(r) = \theta^-(P^-(r))$ are measured in the reference frame S_1 and define monotonic functions

$$\theta^+ : [a(\lambda_2), b(\lambda_2)] \longrightarrow [0, \pi] \qquad \theta^- : [a(\lambda_2), b(\lambda_2)] \longrightarrow [-\pi, 0]$$

such that

$$\theta^+(a(\lambda_2)) = \theta^+(b(\lambda_2)) = \theta^-(a(\lambda_2)) = \theta^-(b(\lambda_2)) = 0\ . \tag{5.9}$$

Finally, denoting by $\Psi(r, \theta) = c_6 + \theta - c_7 \ln r$ the angular coordinate of $R(r, \theta)$ measured in S_2, with θ measured in S_1, let $\Psi^+,\ \Psi^- : [a(\lambda_2), b(\lambda_2)] \longrightarrow \mathbf{R}$ be given by

$$\Psi^+(r) = \Psi(r, \theta^+(r)) \qquad \Psi^-(r) = \Psi(r, \theta^-(r))\ .$$

Again, these are monotonic functions and they satisfy:

$$\Psi^+(a(\lambda_2)) = \Psi^-(a(\lambda_2)) \qquad \text{and} \qquad \Psi^+(b(\lambda_2)) = \Psi^-(b(\lambda_2))\ . \tag{5.10}$$

With this notation, if for some $r_0 \in [a(\lambda_2), b(\lambda_2)]$ we have $\varphi^+(r_0) = \Psi^+(r_0) \pmod{2\pi}$ then the point with S_2 coordinates $(r_0, \varphi^+(r_0))$ is a fixed point for R. Similarly, $\varphi^-(r_0) = \Psi^-(r_0) \pmod{2\pi}$ implies that $(r_0, \varphi^-(r_0))$ is a fixed point for R (see figure 13).

Note that by (5.8) the union of the graphs of φ^+ and φ^- is a connected curve and this curve divides the strip $[a(\lambda_2), b(\lambda_2)] \times \mathbf{R}$ in three connected components. The limited component contains the segment $\{a(\lambda_2)\} \times (-\pi, \pi)$; each one of the unlimited components contains one of the half-lines $\{b(\lambda_2)\} \times (0, +\infty)$ and $\{b(\lambda_2)\} \times (-\infty, 0)$. If either $\Psi^+(a(\lambda_2)) = (2k + 1)\pi$ or

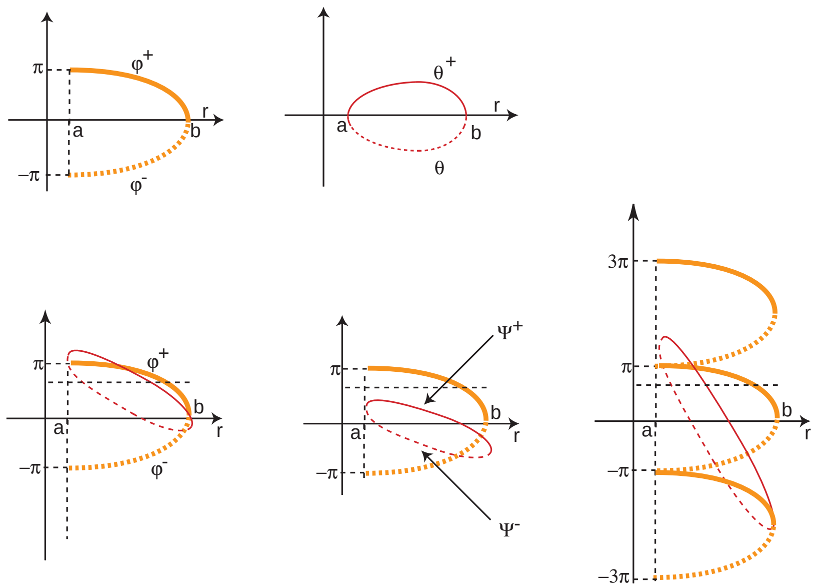

Figure 14: When either $\varphi^+(r) = \Psi^+(r) \pmod{2\pi}$ or $\varphi^-(r) = \Psi^-(r) \pmod{2\pi}$ there is a fixed point for the first return map R. Graphs are: thick lines for $\varphi^\pm$, thin for $\Psi^\pm$, solid lines for +, dashed for -, with $\Psi^+(a(\lambda_2)) \in (-\pi, \pi)$. Left: when $\Psi^+(b(\lambda_2)) > 0$ the graphs of φ^+ and Ψ^+ must cross. At the centre, crossing of the graphs of φ^- and Ψ^- when $\Psi^+(b(\lambda_2)) < 0$. Right: for large λ_2 new fixed points appear in pairs as the graphs of $\Psi^\pm$ cross the graphs of $\varphi^\pm$ several times $\pmod{2\pi}$.

$\Psi^+(b(\lambda_2)) = 2k\pi$ for some $k \in \mathbf{Z}$ then either $(a(\lambda_2), \varphi^+(a(\lambda_2)))$ or $(b(\lambda_2), \varphi^+(b(\lambda_2)))$, respectively, is fixed by R. When this is not the case, let N be an integer such that $\Psi^+(a(\lambda_2)) + 2N\pi \in (-\pi, \pi)$, so $(a(\lambda_2), \Psi^+(a(\lambda_2)) + 2N\pi)$ lies in the limited component of the strip. Since

$$(b(\lambda_2), \Psi^+(b(\lambda_2)) + 2N\pi) = (b(\lambda_2), \Psi^-(b(\lambda_2)) + 2N\pi)$$

lies in one of the unlimited components, then the graphs of Ψ^+ and of Ψ^- must cross the union of the graphs of φ^+ and φ^- (see figure 14). If $(b(\lambda_2), \Psi^+(b(\lambda_2)) + 2N\pi)$ lies in $\{b(\lambda_2)\} \times (0, +\infty)$, then the graph of $\Psi^+(r) + 2N\pi$ crosses the graph of $\varphi^+(r)$, otherwise the graphs of $\Psi^-(r) + 2N\pi$ and of $\varphi^-(r)$ must cross. $\square$

Several periodic trajectories may occur in two ways: first, there may be trajectories that make more than one loop around the place where the original cycle was, appearing as fixed points of some higher iterate R^N of the Poincaré map R; second, the graphs of $\Psi^\pm$ may cross the graphs of $\varphi^\pm$ several times $\pmod{2\pi}$, giving rise to several fixed points of the Poincaré map R. We show next that the second possibility does not take place for small λ_2.

Proposition 14 *For small $\lambda_2 > 0$ the Poincaré map has only one fixed point in $H^{in}_{\mathbf{w}}$.*

Proof: For the map Ψ^+ defined in the proof of proposition 13, using (5.9), we have

$$\Psi^+(b(\lambda_2)) - \Psi^+(a(\lambda_2)) = c_6 + \theta^j(b(\lambda_2)) - c_7 \ln b(\lambda_2) - c_6 - \theta^j(a(\lambda_2)) + c_7 \ln a(\lambda_2) = c_7 \ln \frac{a(\lambda_2)}{b(\lambda_2)} .$$

Then, since by (5.7),

$$\lim_{\lambda_2\to 0} a(\lambda_2) = \lim_{\lambda_2\to 0} b(\lambda_2) = 0 \quad \text{and} \quad \lim_{\lambda_2\to 0} \frac{da}{d\lambda_2}(\lambda_2) = \lim_{\lambda_2\to 0} \frac{db}{d\lambda_2} = 1$$

we get

$$\lim_{\lambda_2\to 0} \left(\Psi^+(b(\lambda_2)) - \Psi^+(a(\lambda_2))\right) = 0$$

even though, since $c_7 > 0$

$$\lim_{\lambda_2\to 0} \Psi^+(b(\lambda_2)) = \lim_{\lambda_2\to 0} \Psi^+(a(\lambda_2)) = \infty \ .$$

It follows that $|\Psi^+(b(\lambda_2)) - \Psi^+(a(\lambda_2))| \ll \pi$ for small $\lambda_2 > 0$ and thus, since $\Psi^\pm$ and $\varphi^\pm$ are monotonic, there is only one crossing $\pmod{2\pi}$ of either the graphs of Ψ^+ and φ^+ or of the graphs of Ψ^- and φ^-. Therefore the fixed point of the Poincaré map is unique. □

5.4 Stability of the fixed point

Proposition 15 *For small $\lambda_2 > 0$ the periodic solution corresponding to the unique fixed point of Poincaré map in $H^{in}_{\mathbf{w}}$ of Proposition 14 is asymptotically stable.*

Proof: We want to estimate the eigenvalues of the derivative $DR(X)$ of the Poincaré map $R : H^{in}_{\mathbf{w}} \longrightarrow H^{in}_{\mathbf{w}}$. To do this we write R as a composition of maps

$$R(X) = P \circ R_* \circ h^{-1}(X)$$

where $R_* = (\rho(r,\varphi), \theta(r,\varphi))$ is the expression (5.5) in polar coordinates, $h(r,\varphi) = (r\cos\varphi, r\sin\varphi)$ and $P(\rho,\theta) = (\rho\cos\theta + \lambda_2, \rho\sin\theta)$. For $X \in H^{in}_{\mathbf{w}}$, $X \neq (0,0)$ we write $h^{-1}(X) = (r(X), \varphi(X))$. From the derivatives

$$DP(\rho,\theta) = \begin{pmatrix} \cos\theta & -\rho\sin\theta \\ \sin\theta & \rho\cos\theta \end{pmatrix} \qquad DR_*(r,\varphi) = \begin{pmatrix} c_5\delta r^{\delta-1} & 0 \\ -\dfrac{c_7}{r} & 1 \end{pmatrix}$$

$$Dh^{-1}(X) = \begin{pmatrix} \cos\varphi(X) & \sin\varphi(X) \\ -\dfrac{\sin\varphi(X)}{r(X)} & \dfrac{\cos\varphi(X)}{r(X)} \end{pmatrix}$$

it follows that $DR(X)$ does not depend explicitly on λ_2. Then, at $X = h^{-1}(r,\varphi)$ we have

$$\det DR(X) = c_5^2\delta r^{2\delta-2}(X) \ .$$

The trace $\operatorname{tr} DR(X)$, omitting the dependence on X, is given by

$$\operatorname{tr} DR(X) = \left(c_5\delta r^{\delta-1} + \frac{\rho}{r}\right)(\cos\theta\cos\varphi + \sin\theta\sin\varphi) + \frac{c_7\rho}{r}(\sin\theta\cos\varphi - \cos\theta\sin\varphi) \ .$$

We want to estimate $\det DR$ and $\operatorname{tr} DR$ at points $X(\lambda_2)$ where $R(X(\lambda_2)) = X(\lambda_2)$ for small $\lambda_2 > 0$. In polar coordinates we get $h^{-1}(X(\lambda_2)) = (r(\lambda_2), \varphi(\lambda_2))$ and we know that $\lim_{\lambda_2\to 0} r(\lambda_2) = 0$. Then from the expression above, and since by (5.6) we have $\delta > 1$,

$$\lim_{\lambda_2\to 0} \det DR(X)(\lambda_2) = 0 \ .$$

For the trace, substituting the value of $\rho(r,\varphi) = c_5 r^\delta$ obtained in (5.5) we get

$$\lim_{r\to 0} \frac{\rho(r,\varphi)}{r} = \lim_{r\to 0} c_5 r^{\delta-1} = 0$$

since $\delta > 1$. Then at the limit cycle $\lim_{\lambda_2\to 0} \operatorname{tr} DR(X(\lambda_2)) = 0$. It follows that the eigenvalues of $DR(X(\lambda_2))$ also tend to zero and thus for small λ_2 they lie within the disk of radius 1. □

6 Proof of theorem 7: existence of homoclinic dynamics of Shilnikov type

In general, vector fields with homoclinic cycles are structurally unstable and present fast transitions between different (and complex) dynamics. In this section, we are assuming that both symmetries $\mathbf{Z}_2(\gamma_1)$ and $\mathbf{Z}_2(\gamma_2)$ are broken (i.e. $\lambda_1 \neq 0$ and $\lambda_2 \neq 0$) and that property (P8) is satisfied. Without loss of generality, we assume that the transition map from $\mathbf{v}$ to $\mathbf{w}$ is just a translation along the horizontal axis. Recall that the parameter λ_2 controls the splitting of the heteroclinic orbit $[\mathbf{v} \to \mathbf{w}]$ and λ_1 is the parameter controlling *the angle* in $H^{in}_{\mathbf{v}}$ of the transverse intersection $W^u(\mathbf{w})$ and $W^s(\mathbf{v})$.

Near the heteroclinic network $\Sigma^\star$ which exists for $\lambda_1 \neq 0$ and $\lambda_2 = 0$, there exists an invariant Cantor set topologically equivalent to a full shift with an infinite countable set of periodic solutions. It corresponds to infinitely many intersections of a vertical rectangle $\mathcal{R}_{\mathbf{v}}$ in $H^{in}_{\mathbf{v}}$ with its image, under the first return map to $H^{in}_{\mathbf{v}}$. Only a finite number of them will survive, under a small perturbation (i.e., the horseshoes which exist for $\lambda_2 = 0$ lose infinitely many *legs*).

If $\lambda_1 \neq 0 \neq \lambda_2$, the tips of the spirals $\Phi^{-1}_{\mathbf{w}}(W^s(\mathbf{v})) \cap H^{in}_{\mathbf{w}}$ and $\Psi_{\mathbf{v},\mathbf{w}} \circ \Phi_{\mathbf{v}}(W^u(\mathbf{w})) \cap H^{in}_{\mathbf{w}}$ are separated and generically the center of the first curve does not intersect the second spiral. Thus, the spirals have only a finite number of intersections and consequently the number of heteroclinic connections from $\mathbf{v}$ to $\mathbf{w}$ is finite.

For $\lambda_1 \neq 0 \neq \lambda_2$, besides the existence of uniformly hyperbolic horseshoes, there are homoclinic orbits of $\mathbf{v}$ and $\mathbf{w}$, whose coexistence we address in the present section. The existence of these homoclinic loops is a phenomenon which depends on the right combination of the parameters (λ_1, λ_2).

We start by a global description of $\Phi^{-1}_{\mathbf{w}}(W^s(\mathbf{v})) \cap H^{in}_{\mathbf{w}}$. The homoclinic connections are then discussed separately: those in $\mathbf{v}$ in section 6.1 and those in $\mathbf{w}$ in section 6.2. For λ_1 close to zero, we are assuming that $W^s(\mathbf{v})$ intersects the wall $H^{out}_{\mathbf{w}}$ of the cylinder W in an ellipsis. This is the expected unfolding from the coincidence of the invariant manifolds of the equilibria (see figure 15).

We are assuming that $W^u(\mathbf{w}) \cap W^s(\mathbf{v}) \cap H^{out}_{\mathbf{w}}$ consists of two points P_1 and P_2 (see figure 15). Each of these points $W^s(\mathbf{v}) \cap H^{out}_{\mathbf{w}}$ defines a segment and each segment may be approximated by a line of slope $\pm\lambda_1$ parametrized by s (see figure 16) with either $s \in (0, \varepsilon^*)$ or $s \in (\pi - \varepsilon^*, \pi)$, respectively, where $\varepsilon^* \in (0, \varepsilon)$. The points are $\mathbf{Z}_2$–related; this is an artifact of the broken symmetry.

Near P_1, the slope is λ_1; near P_2, the slope is $-\lambda_1$. When $\lambda_1 = 0$, the invariant manifolds coincide; when $\lambda_1 \neq 0$, these two segments appear automatically. For assumption, we have:

$$\lim_{s\to 0^+} s_1(s) = P_1 \quad \text{and} \quad \lim_{s\to \pi^-} s_2(s) = P_2.$$

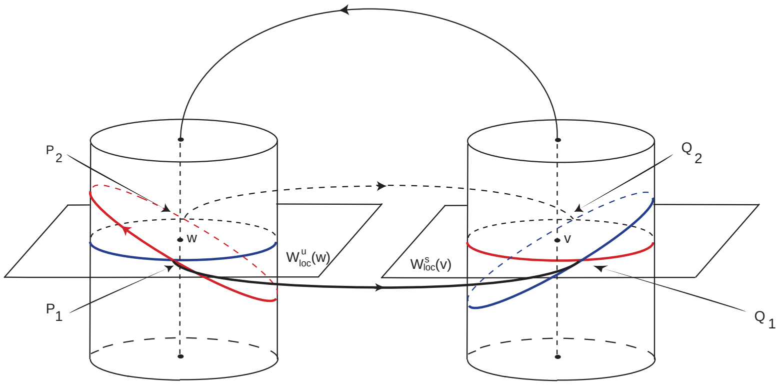

Figure 15: Both $W^s(\mathbf{v}) \cap H^{out}_{\mathbf{w}}$ and $W^u(\mathbf{w}) \cap H^{in}_{\mathbf{v}}$ are closed curves, approximated by ellipses for small λ_1.

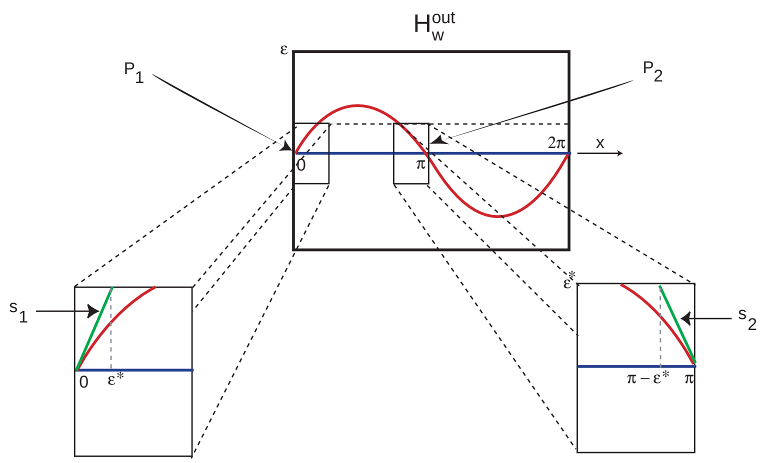

Figure 16: The cylinder $H^{out}_{\mathbf{w}}$ is shown here opened into a rectangle to emphasize the fact that locally $W^s(\mathbf{v})$ defines two lines on this wall.

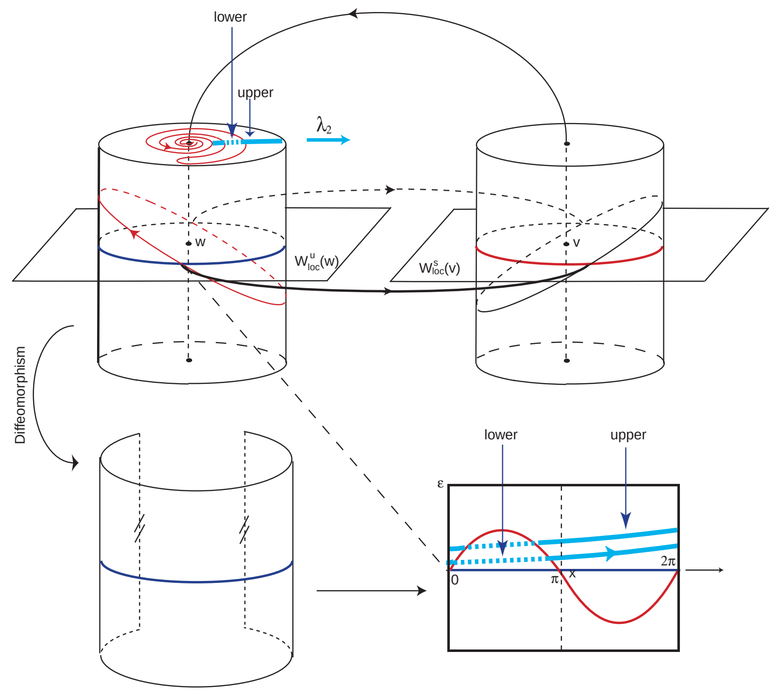

Figure 17: The backwards iterate $\Phi_{\mathbf{w}}^{-1}(W^s(\mathbf{v}))$ consists of two joined-up spirals in $H^{in}_{\mathbf{w}}$ shown in red, that divide $H^{in}_{\mathbf{w}}$ in two components, mapped into the upper and lower parts of $H^{in}_{\mathbf{v}}$. As λ_2 increases from zero, $W^u(\mathbf{v}) \cap H^{in}_{\mathbf{w}}$ moves along the thick blue line (grey in print), whose image by $\Phi_{\mathbf{w}}$ describes a helix in $H^{out}_{\mathbf{w}}$. Arrows on $W^s(\mathbf{v})$ and on the blue line are just indications of orientation, not of flow.

By lemma 10, locally the curves $\Phi_{\mathbf{w}}^{-1}(s_1(s))$ and $\Phi_{\mathbf{w}}^{-1}(s_2(s))$ are disjoint spirals in $H^{in}_{\mathbf{w}}$ accumulating on the point $W^s_{loc}(\mathbf{w}) \cap H^{in}_{\mathbf{w}}$.

Globally, $W^s(\mathbf{v}) \cap H^{out}_{\mathbf{w}}$ is a closed curve $(x(s), y(s))$, $s \in [0, 2\pi]$, with two arcs where $y(s)$ is monotonic. Each arc is mapped diffeomorphically by $\Phi_{\mathbf{w}}^{-1}$ into a spiral and the two spirals meet at the image of the maximum of $y(s)$ (see figure 17).

6.1 Homoclinic connections of v - Tongues of Attracting Periodic Trajectories

Althought the existence of homoclinic orbits is not easy to prove, here we have been able to characterize the curves for which we observe homoclinic cycles (of Shilnikov type) arising in the unfolding of the heteroclinic network $\Sigma^\star$. Our study is consistent with the exhaustive study of bifurcations arising in the unfolding of Bykov cycles done in [20] and [31].

Note that we are assuming that $\alpha_{\mathbf{v}}, \alpha_{\mathbf{w}} > 0$ since hypothesis (P8) is satisfied. The primary homoclinicity of $\mathbf{v}$ occurs when the unstable manifold of $\mathbf{v}$ has a successful encounter with the stable manifold of the same equilibrium on $H^{in}_{\mathbf{w}}$. Here, we will find the values $\lambda_2(\mathbf{v})$ of the parameter λ_2 for which system (2.2) has a homoclinic connection of $\mathbf{v}$. This happens when $\lambda_1 > 0$ and either:

$$\lambda_2(\mathbf{v}) = \left(\frac{\lambda_1 s}{c_4}\right)^{\frac{1}{\delta_{\mathbf{w}}}} \quad \text{and} \quad s - c_3 + \left(\frac{\alpha_{\mathbf{w}}}{C_{\mathbf{w}}}\right) \ln\left(\frac{\lambda_1 s}{c_4}\right) = 2k\pi, \quad k \in \mathbf{Z} \tag{6.11}$$

or

$$\lambda_2(\mathbf{v}) = \left(-\frac{\lambda_1(s-\pi)}{c_4}\right)^{\frac{1}{\delta_{\mathbf{w}}}} \quad \text{and} \quad s - c_3 + \left(\frac{\alpha_{\mathbf{w}}}{C_{\mathbf{w}}}\right) \ln\left(\frac{-\lambda_1(s-\pi)}{c_4}\right) = 2k\pi, \quad k \in \mathbf{Z}. \quad (6.12)$$

Using the above equations, we may write the parameter λ_1^k as function of λ_2:

$$\lambda_1^k(\lambda_2) = \frac{c_4 \lambda_2^{\delta_{\mathbf{w}}}}{2k\pi + c_3 - \frac{\alpha_{\mathbf{w}}}{E_{\mathbf{w}}} \ln(\lambda_2)} \quad \text{and} \quad s \in (0, \varepsilon^\star) \quad (6.13)$$

or

$$\lambda_1^k(\lambda_2) = \frac{c_4 \lambda_2^{\delta_{\mathbf{w}}}}{\pi + 2k\pi + c_3 - \frac{\alpha_{\mathbf{w}}}{E_{\mathbf{w}}} \ln(\lambda_2)} \quad \text{and} \quad s \in (\pi - \varepsilon^\star, \pi) \quad (6.14)$$

Both equations (6.13) and (6.14) may be simplified as:

$$\lambda_1^k(\lambda_2) = \frac{c_4 \lambda_2^{\delta_{\mathbf{w}}}}{k\pi + c_3 - \frac{\alpha_{\mathbf{w}}}{E_{\mathbf{w}}} \ln(\lambda_2)}$$

where the denominator is either for the value of s or of $\pi - s$ and only has meaning when it lies in the interval $(0, \varepsilon^*)$. For $\lambda_2 > 0$, define:

$$k_0(\lambda_2) = \min\left\{k \in \mathbf{Z} : 2k\pi + c_3 - \frac{\alpha_{\mathbf{w}}}{E_{\mathbf{w}}} \ln(\lambda_2) > 0\right\}.$$

Further, we will use the information of the next lemma to depict the bifurcation diagram of figure 18.

Lemma 16 *1.* $\lim_{\lambda_2 \to 0} k_0(\lambda_2) = -\infty$

2. $\forall k > k_0, \quad \frac{d\lambda_1^k}{d\lambda_2}(0) = 0$*;*

Proof:

1. It is immediate from the fact that when $\lambda_2 \to 0$, $\ln(\lambda_2) \to -\infty$.

2. Since $\delta_{\mathbf{w}} > 1$, observe that:

$$\frac{d\lambda_1^k}{d\lambda_2}(\lambda_2) = \frac{c_4 \lambda_2^{\delta_{\mathbf{w}}-1}}{k\pi + c_3 - \frac{\alpha_{\mathbf{w}}}{E_{\mathbf{w}}} \ln(\lambda_2)} + \frac{c_4 \lambda_2^{\delta_{\mathbf{w}}-1} \frac{\alpha_{\mathbf{w}}}{E_{\mathbf{w}}}}{\left(k\pi + c_3 - \frac{\alpha_{\mathbf{w}}}{E_{\mathbf{w}}} \ln(\lambda_2)\right)^2}.$$

When $\lambda_2 \to 0$, the above expression tends to zero.

□

In a neighbourhood of the singular point $(\lambda_1, \lambda_2) = (0, 0)$, the graph of λ_1 as function of λ_2 is depicted in figure 18, for different values of $k > k_0$. Recall that $s \in [0, \varepsilon^\star]$; in particular, the end points of the graphs coincide with the intersection of the graphs of $\lambda_1^k(\lambda_2)$ with that of $\lambda_1(\lambda_2) = \frac{c_4 \lambda_2^{\delta_{\mathbf{w}}}}{\varepsilon^\star}$ (which represents the evolution of the end point of s_i of the linear approximation of $W^s(\mathbf{v}) \cap H_{\mathbf{w}}^{out,+}$). When $\lambda_2 \to 0^+$, the equation

$$k\pi + c_3 - \frac{\alpha_{\mathbf{w}}}{E_{\mathbf{w}}} \ln(\lambda_2) = 0$$

has infinitely many solutions (one for each k). In particular:

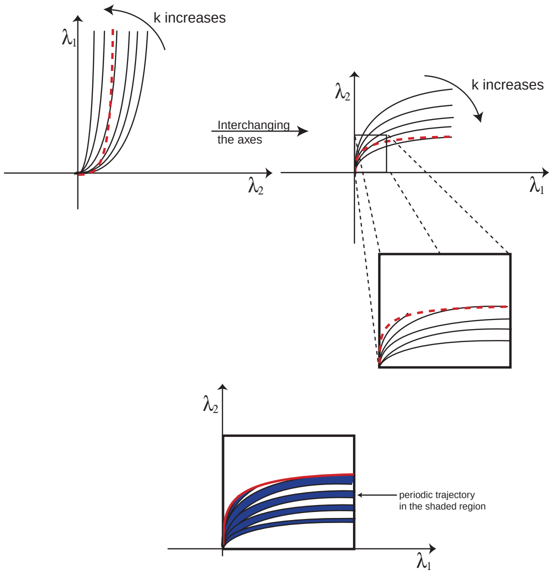

Figure 18: Top: solid lines are the curves $(\lambda_1^k(\lambda_2), \lambda_2)$ where there is a homoclinic connection to $\mathbf{v}$, dashed line is the limit $s = \varepsilon^*$ for the linear approximation of $W^s(\mathbf{v}) \cap H_{\mathbf{w}}^{out}$. Bottom: Pairs of these lines delimitate a tongue where there is a periodic trajectory.

Lemma 17 *For all k sufficiently large, there exists $\lambda_2^\star(k)$ such that*

$$\lim_{\lambda_2 \to \lambda_2^\star(k)} \lambda_1^k(\lambda_2) = +\infty$$

and moreover $\lim_{k\to+\infty} \lambda_2^\star(k) = 0$. In other words, the graph of $\lambda_1^k(\lambda_2)$ has a vertical asymptote for $\lambda_2 = \lambda_2^\star(k)$.

Observing closer the bifurcation diagram of figure 18, it follows that for a fixed λ_2, there are finitely many λ_1 for which we observe homoclinic connections of $\mathbf{v}$. We also conclude that for a fixed λ_2, there exists a $\lambda_1^\star$, such that for $\lambda_1 < \lambda_1^\star$, there are no more homoclinic connections.

Remark 3 *Note that the eigenvalues of $\mathbf{v}$ verify $C_{\mathbf{v}} > E_{\mathbf{v}}$ and consequently the spectral assumption of the attracting Shilnikov problem holds. For small variations of the parameters, the equilibria are persistent and the same conditions on the eigenvalues are satisfied.*

Assertions 1. and 2. of theorem 7 follow from lemmas 16 and 17. The other assertions of theorem 7 follow from the results of Shilnikov [38], Glendinning and Sparrow [19] and Shilnikov *et al* [39, 40].

Corollary 18 *In the bifurcation diagram (λ_1, λ_2), there are infinitely many tongues of attracting periodic trajectories accumulating on the line $\lambda_2 = 0$. These periodic trajectories bifurcate from the attracting homoclinic orbit of $\mathbf{v}$.*

It is straightforward that when $\lambda_2 \to 0$, the homoclinic orbits of $\mathbf{v}$ accumulate on the heteroclinic connection $[\mathbf{v} \to \mathbf{w}]$.

6.2 Homoclinic orbits of w - A cascade of horseshoes is only a participating part!

In three-dimensions, the simplest homoclinic cycle that yield infinitely many transitions between complicated dynamics is the classical Shilnikov problem (unstable version). In this section, we prove the existence of homoclinic orbits in a neighbourhood of the ghost of the heteroclinic network $\Sigma^\star$. Near these trajectories, there are infinitely many suspended horseshoes. When the vector field is perturbed, generically the homoclinic orbits are destroyed and we conjecture that persistent strange attractors might coexist. Among these sets, we are able to prove that along specific curves in the bifurcation diagram, homoclinic trajectories of $\mathbf{w}$ exist.

Using the same argument as before, we assume the existence of two segments r_1 and r_2 (parametrized by s) which correspond to a linear approximation of $W^u(\mathbf{w}) \cap H_{\mathbf{v}}^{in}$, in a neighbourhood of the points $W^s(\mathbf{v}) \cap W^u(\mathbf{w}) \cap H_{\mathbf{v}}^{in}$ (Q_1 and Q_2). The parameter $\lambda_1 > 0$ is the absolute value of the slope of r_1 and r_2; (near Q_1, the slope is λ_1; near Q_2, the slope is $-\lambda_1$). Their parametrizations are given by:

$$r_1 : \quad r_1(s) = (s, \lambda_1 s), \quad \text{for} \quad s \in [0, \varepsilon^\star]$$

and

$$r_2 : \quad r_2(s) = (s, -\lambda_1(s-\pi)), \quad \text{for} \quad s \in [\pi - \varepsilon^\star, \pi].$$

As before, we have:

Lemma 19 *If $\lambda_1 \neq 0$, then $\phi_{\mathbf{v}}(r_1(s))$ and $\phi_{\mathbf{v}}(r_2(s))$ are disjoint logarithmic spirals in $H_{\mathbf{v}}^{out}$ accumulating on the point $W_{loc}^u(\mathbf{v}) \cap H_{\mathbf{v}}^{out}$.*

Observing that:

$$\phi_{\mathbf{v}}(r_1(s)) = \phi_{\mathbf{v}}(s, \lambda_1 s) = (c_1(\lambda_1 s)^{\delta_{\mathbf{v}}}; -g_{\mathbf{v}} \ln(\lambda_1 s) + s + c_2) = (\sigma, \phi)$$

and

$$\phi_{\mathbf{v}}(r_2(s)) = \phi_{\mathbf{v}}(s, -\lambda_1(s-\pi)) = (c_1(-\lambda_1(s-\pi))^{\delta_{\mathbf{v}}}; -g_{\mathbf{v}} \ln(-\lambda_1(s-\pi)) + s + c_2) = (\sigma, \phi),$$

the homoclinic orbit associated to $\mathbf{w}$ (investigated on H_w^{in}) exists if and only if either

$$\lambda_2(\mathbf{w}) = c_1(\lambda_1 s)^{\delta_{\mathbf{v}}} \quad \text{and} \quad s + c_2 - \left(\frac{\alpha_{\mathbf{v}}}{E_{\mathbf{v}}}\right) \ln(\lambda_1 s) = 2k\pi, k \in \mathbf{Z} \tag{6.15}$$

or

$$\lambda_2(\mathbf{v}) = c_1\left(-\lambda_1(s-\pi)\right)^{\delta_{\mathbf{v}}} \quad \text{and} \quad s + c_2 - \left(\frac{\alpha_{\mathbf{v}}}{C_{\mathbf{v}}}\right) \ln\left(-\lambda_1(s-\pi)\right) = 2k\pi, k \in \mathbf{Z}. \tag{6.16}$$

Using the above equations, we may write the parameter λ_1^k as function of λ_2 as either:

$$\lambda_1^k(\lambda_2) = \frac{c_1^\star \lambda_2^{\frac{1}{\delta_{\mathbf{v}}}}}{2k\pi + c_2 - \frac{\alpha_{\mathbf{v}}}{E_{\mathbf{v}}}\ln(\lambda_2)} \quad \text{and} \quad s \in (0, \varepsilon^\star)$$

or

$$\lambda_1^k(\lambda_2) = \frac{c_1^\star \lambda_2^{\frac{1}{\delta_{\mathbf{v}}}}}{\pi + 2k\pi + c_2 - \frac{\alpha_{\mathbf{v}}}{E_{\mathbf{v}}}\ln(\lambda_2)} \quad \text{and} \quad s \in (0, \varepsilon^\star).$$

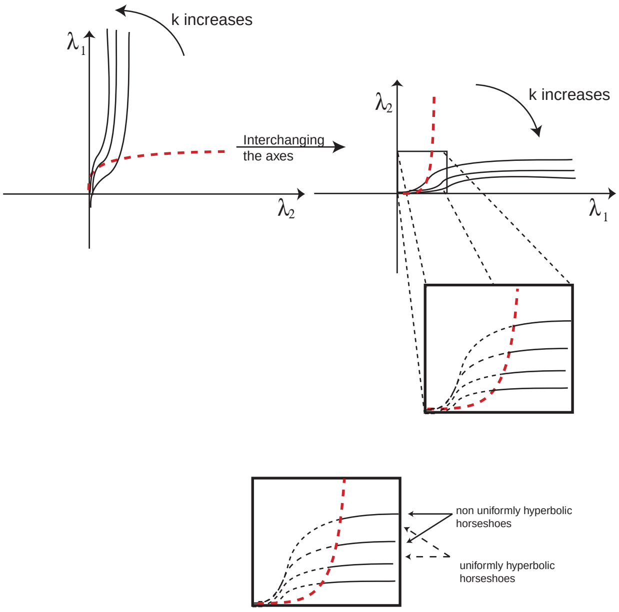

Figure 19: Top: Solid lines are the curves $(\lambda_1^k(\lambda_2), \lambda_2)$ where there is a homoclinic connection to $\mathbf{w}$, dashed line is the limit $s = \varepsilon^*$ for the linear approximation of $W^u(\mathbf{w}) \cap H_{\mathbf{v}}^{in}$. Bottom: at each one of these lines a horseshoe is created.

The proof of theorem 8 proceeds as that of Theorem 7, except that the curves $(\lambda_1^k(\lambda_2), \lambda_2)$ are tangent to the λ_1–axis (see figure 19). It follows from results of Shilnikov [38] and Glendinning and Sparrow [19], that a horseshoe bifurcates from each homoclinic connection. In the neighbourhood of these homoclinic orbits, infinitely many periodic solutions of saddle type occur. These solutions are contained in suspended horseshoes that accumulate on the homoclinic cycle, whose dynamics is conjugated to a subshift of finite type on an infinite number of symbols. Multipulse homoclinic orbits and attracting 2-periodic solutions may unfold from the homoclinic cycles, under additional hypothesis $(E_{\mathbf{w}} - 2C_{\mathbf{w}} < 0)$.

Remark 4 *Besides the interest of the study of the dynamics arising in generic unfoldings of an attracting heteroclinic network, its analysis is important because in the fully non-equivariant case (at first glance) the return map seems intractable. Here we are able to predict qualitative features of the dynamics of the perturbed vector field by assuming that the perturbation is very close to the organizing center. This is an important advantage of studying systems close to symmetry.*

References

[1] L. Abramov, *On the entropy of a flow* (Russian), Dokl. Akad. Nauk. SSSR 128, 873–875, 1959

[2] M. Aguiar, *Vector Fields with heteroclinic networks,* PhD Thesis, Departamento de Matemática Aplicada, Faculdade de Ciências da Universidade do Porto, 2003

[3] M. Aguiar, S. B. Castro and I. S. Labouriau, *Dynamics near a heteroclinic network,* Nonlinearity, No. 18, 391–414, 2005

[4] M. Aguiar, S. B. Castro and I. S. Labouriau, *Simple Vector Fields with Complex Behaviour*, Int. Jour. of Bifurcation and Chaos, Vol. 16, No. 2, 369–381, 2006

[5] M. Aguiar, I. S. Labouriau and A. Rodrigues, *Swicthing near a heteroclinic network of rotating nodes*, Dynamical Systems: an International Journal, Vol. 25, Issue 1, 75–95, 2010

[6] A. A. Andronov, E. A. Leontovich, I. I. Gordon, A. G. Maier, *Theory of bifurcations of dynamical systems on a plane*, Israel Program of Scientific Translations, Jerusalem, 1973

[7] D. V. Anosov, S. Kh. Aranson, V. I. Arnold, I. U. Bronshtein, V. Z. Grines and Yu. S. Il'yashenko, *Ordinary Differential Equations and Smooth Dynamical Systems*, Springer, 1988

[8] F. H. Busse, K. E. Heikes, *Convection in a rotating layer: A simple case of turbulence*, Science, 208 (4440), 173-175, 1980

[9] V. V. Bykov, *Orbit Structure in a Neighbourhood of a Separatrix Cycle Containing Two Saddle-Foci*, Amer. Math. Soc. Transl, Vol. 200, 87–97, 2000

[10] P. Channell, G. Cymbalyuk and A. Shilnikov, *Origin of Bursting through Homoclinic Spike Adding in a Neuron Model*, Physical Review Letters, PRL 98, 134101–134105, 2007

[11] J. B. van den Berg, S. A. van Gils and T. P. P. Visser, *Parameter dependence of homoclinic solutions in a single long Josepson junction*, Nonlinearity, No. 16(2), 707–717, 2003

[12] V. Carmona, F. F. Sánchez and A. E. Teruel, *Existence of a reversible T-point heteroclinic cycle in a piecewise linear version of the Michelson system*, SIAM J. Applied Dynamical Systems, 1032–1048, 2008

[13] P. Chossat, *Forced reflectional symmetry breaking of an O(2)-symmetric homoclinic cycle*, Nonlinearity, Vol. 70, Issue 2, 297–310, 1996

[14] F. Fernández-Sanchez, *Comportamiento dinámico y de bifurcationes en algunas conexiones globales de equilíbrio en sistemas tridimensionales*, Ph.D. Thesis, University of Sevilla, 2002

[15] F. Fernández-Sánchez, E. Freire and A. J. Rodríguez-Luis, *T-Points in a* $\mathbf{Z}_2$*-Symmetric Electronic Oscillator. (I) Analysis*, Nonlinear Dynamics, 28, 53–69, 2002

[16] J. Franks and R. F. Williams, *Entropy and Knots*, Transactions of the American Mathematical Society, Vol. 291, No. 1, 241–253, 1985

[17] P. Gaspard, *Generation of a countable set of homoclinic flows through bifurcation*, Phys. Letters, 97 A, Issues 1–2, 1–4 , 1983

[18] P. Glendinning, J. Abshagen and T. Mullin, *Imperfect Homoclinic Bifurcation*, Phys. Rev. E 64, 036208–036215, 2001

[19] P. Glendinning and C. Sparrow, *Local and global behavior near homoclinic orbits*, J. Stat. Phys., 35, 645–696, 1984

[20] P. Glendinning and C. Sparrow, *T-points: A codimension Two Heteroclinic Bifurcation*, J. Stat. Phys., 43, No. 3–4, 479–488, 1986

[21] M. I. Golubitsky, I. Stewart, and D. G. Schaeffer, *Singularities and Groups in Bifurcation Theory* , Vol. II, Springer, 2000

Math. Proc. Camb. Phil. Soc, 103, 189–192, 1988

[22] M. Hirasawa and E. Kin, *Determination of generalized horseshoe map inducing all links*, Topology and its Applications, 139, No. 1–3, 261–277, 2004

[23] A. J. Homburg and J. Knobloch, *Switching homoclinic networks*, Dynamical Systems: an International Journal, Vol. 25, Issue 3, 351–358, 2010

[24] A. J. Homburg and M. A. Natiello, *Accumulations of T-points in a model for solitary pulses in an excitable reaction-diffusion medium*, Physica D, Vol. 201, No. 3–4, 212–229, 2005

[25] S. Ibáñez and J. A. Rodríguez, *Shilnikov configurations in any generic unfolding of the nilpotent singularity of codimension three in* $\boldsymbol{R}^3$, Journal of Differential Equations, 208, 147–175, 2008

[26] A. Katok and B. Hasselblatt, *Introduction to the Modern Theory of Dynamical Systems*, Cambridge University Press, Cambridge, 1995

[27] E. Kin, *The third power of the Smale horseshoe induces all link types*, J. Knot Theory Ramifications, Vol. 9, No. 7, 939–953, 2000

[28] V. Kirk and A. M. Rucklidge, *The effect of symmetry breaking on the dynamics near a structurally stable heteroclinic cycle between equilibria and a periodic orbit,* Dynamical Systems: An International Journal, Vol. 23, Nr.1, 41–83, 2008

[29] J. Knobloch, T. Riez, M. Vielits, *Nonreversible Homoclinic Snaking*, Pre-print, 2010

[30] M. Krupa, and I. Melbourne, *Asymptotic Stability of Heteroclinic Cycles in Systems with Symmetry,* Ergodic Theory and Dynam. Sys., Vol. 15, 121–147, 1995

Soc. Edinburgh, 134A, 1177–1197, 2004

[31] J. S. W. Lamb, M. A. Teixeira, Kevin N. Webster *Heteroclinic bifurcations near Hopf-zero bifurcation in reversible vector fields in* $\mathbf{R}^3$, Journal of Differential Equations, 219, 78–115, 2005

[32] I. Melbourne, *Intermittency as a codimension three phenomenon*, J. Dyn. Stab. Syst., 1, 347–367, 1989

[33] I. Melbourne, M. R. E. Proctor and A. M. Rucklidge, *A heteroclinic model of geodynamo reversals and excursions*, Dynamo and Dynamics: a Mathematical Challenge, Kluwer, Dordrecht, 2001

[34] L. Mora, M. Viana, *Abundance of strange attractors*, Acta Math. 171, 1–71, 1993

[35] Z. Ren and J. Yang, *On the* C^1*–normal forms for hyperbolic vector fields*, C. R. Acad. Sci. Paris, Ser.I 336, Issue 9, 709–712, 2003

[36] A. A. P. Rodrigues, I. S. Labouriau, M. A. D. Aguiar, *Chaotic Double Cycling*, Dynamical Systems: an International Journal, Vol. 26, Issue 2, 199–233, 2011

[37] V. S. Samovol, *Linearization of a system of differential equations in the neighbourhood of a singular point,* Sov. Math. Dokl, Vol. 13, 1255–1959, 1972

[38] L. P. Shilnikov, *A case of the existence of a countable number of periodic motions*, Sov. Math. Dokl., 6, 163–166, 1965

[39] L. P. Shilnikov, A. L. Shilnikov, D. M. Turaev, and L. U. Chua, *Methods of Qualitative Theory in Nonlinear Dynamics*, Part I, World Scientific Publishing Co., 1998

[40] L. P. Shilnikov, A. L. Shilnikov, D. M. Turaev, and L. U. Chua, *Methods of Qualitative Theory in Nonlinear Dynamics*, Part II, World Scientific Publishing Co., 2001

[41] S. Wiggins, *Global Bifurcations and Chaos: Analytical Methods*, Springer-Verlag, 1988

[42] Y. Xiao-feng, G. Rui-hai, *Coexistence of the Chaos and the Periodic Solutions in Planar Fluids Flows*, Applied Mathematics and Mechanics (English version), Vol. 12, N. 12, 1135–1142, 1991

[43] J. A. Yorke, K. T. Alligood, *Period-Doubling Cascade of Attractors: A prerequisite for Horseshoes*, Communications in Mathematical Physics, 101, 305–321, 1985